Spring 2017

Evaluation of non-chromate passivations on electroplated γ-phase zinc nickel

Steven Michael Volz

Department:

EVALUATION OF NON-CHROMATE PASSIVATIONS ON ELECTROPLATED γ-PHASE ZINC NICKEL

by

STEVEN MICHAEL VOLZ

A THESIS

Presented to the Faculty of the Graduate School of the

MISSOURI UNIVERSITY OF SCIENCE AND TECHNOLOGY

In Partial Fulfillment of the Requirements for the Degree

MASTER OF SCIENCE IN MATERIALS SCIENCE AND ENGINEERING

2017

Approved by

Matthew J. O'Keefe, Advisor
William G. Fahrenholtz, Advisor
Mark E Schlesinger

PUBLICATION THESIS OPTION

This thesis has been prepared in the format used by the publication *Surface Engineering.* Both papers contained in this thesis will be submitted for publication as follows:

Paper I pages 24-47 are intended for submission to *Surface Engineering.*

Paper II pages 48-69 are intended for submission to *Transactions of the Institute of Metal Finishing*.

ABSTRACT

This research focused on the corrosion response and electrochemical behavior of electroplated low hydrogen embrittlement alkaline γ-phase zinc nickel with passivation layers. The motivation was the need to replace hexavalent chromium conversion coatings in military grade electrical systems with a more environment friendly alternative. The passivation layers were employed for the purpose of mitigating corrosion attack while maintaining low contact resistance. Trivalent chromium-based passivations and cerium-based passivations were compared against the currently used hexavalent chromium conversion coating. The coating systems were compared using electrochemical impedance spectroscopy, cyclic potentiodymanic scans, salt spray exposure testing, electrical resistance measurements, microstructure analysis, and compositional analysis. Coating systems with lower open circuit had a lower corrosion current and performed better during salt spray testing. All of the systems evaluated had corrosion products consistent with oxidized zinc compounds but the morphology of the passivation was dependent on the passivation. The electrical contact resistance ranged from 1 to 10^8 mΩ/cm^2, after salt spray testing. Two versions of Trivalent chromium-based passivations, were able to meet military performance specifications after corrosion testing.

ACKNOWLEDGEMENTS

I would like thank my advisors, Dr. William Fahrenholtz and Dr. Matthew O'Keefe, first and foremost for providing me with this amazing opportunity and for providing me with their guidance throughout my graduate studies. Second, I would also like to acknowledge James Claypool for his help with many aspects of this research and for being there to help me understand several difficult concepts in this work. Next a great thanks to Dr. Mark Schlesinger for serving on my committee.

Next I would like to acknowledge Dr. Eric Bohannan, Dr. Clarissa Wisner, and Ron Hass for providing access to much of the equipment and tools used in this research. Without them much of this work would be impossible.

I would also like to thank my parents, Mike and Laurie Volz, for their amazing love and support during this journey, and my significant other, Katherine Baker, for giving me a daily push to strive to be my best and to get through the more difficult times. And to all of my friends thank you for giving many memorable times during my time in graduate school.

Finally, I would like to acknowledge the Strategic Environmental Research and Development Program (SERDP) for the support necessary to complete this project through project SEED WP-2527.

TABLE OF CONTENTS

Page

PAPER

LIST OF ILLUSTRATIONS

SECTION Page

LIST OF TABLES

SECTION

1. INTRODUCTION

1.1 RESEARCH OBJECTIVE

Department of Defense electrical system interconnects is currently provided by electroplated cadmium passivated with a chromate conversion coating (CrCC) for low contact resistance corrosion protection. An electroplated low hydrogen embrittlement γ-phase zinc nickel alloy (γ-ZnNi) has been determined to be a suitable replacement for electroplated cadmium coatings due to galvanic compatibility, being compatible with low hydrogen embrittlement bake procedures, and meeting other military performance requirements.[1] The chromate conversion coating, however, is still the only commercial available passivation that has been approved with γ-ZnNi for electrical connectors used in U.S. Department of Defense applications.[1] The objective of this research was to develop and evaluate non-hexavalent passivations on γ-ZnNi. The passivations studied were trivalent chromium-based (TCP) and cerium-based conversion coatings (CeCC). Both types of passivations have been shown to increase the corrosion resistance of the metallic substrates.[2-3] Investigation into use of TCP and CeCC passivations on γ-ZnNi for electrical connector applications was the focus of this work.

This research was done to answer several questions. First, can CeCCs and TCPs improve the corrosion performance of γ-ZnNi? Second, can either CeCCs or TCP-based passivations provide similar or better corrosion protection than CrCCs? Third, can these passivations provide the desired corrosion resistance while maintaining the needed electrical contact resistance? These questions were answered using several characterization methods. The electrochemical response was studied using both cyclic potentiodynamic

scans and electrochemical impedance spectroscopy. These methods gave insight into the corrosion behavior of the coating systems such as corrosion resistance, and electrochemical changes within the systems. These tests allowed for evaluation of the systems in less than one day before the weeks of salt spray testing. Exposure to ASTM B117 neutral salt spray conditions was used to observe corrosion performance under accelerated test conditions. Electrical contact resistance was measured in accordance with the MIL-DTL-81706 specification. The coating systems microstructures and chemical compositions were characterized using scanning electron microscopy, energy dispersive X-ray spectroscopy and X-ray diffraction. The papers that make up the main chapters of this thesis discuss the results and answer the questions above.

1.2 PAPER DESCRIPTIONS

The intended journal for Paper I is *Surface Engineering.* The first paper characterized passivation coatings on γ-ZnNi using electrochemical methods and also examined the corrosion response and contact resistance of the passivations. The paper used cyclic potentiodynamic scans (CPDS) and electrochemical impedance spectroscopy (EIS) to compare the different coating system electrochemical responses. CPDS revealed that the cerium-based passivations (CeCC) had more cathodic corrosion potentials, at -670 mV, than the trivalent chromium-based passivations (-720 to -860 mV). The corrosion current for TCP was 105 $\mu A/cm^2$, while the CeCCs had corrosion currents ranging from 56 to 170 $\mu A/cm^2$. The results were then compared to the salt spray testing (SST) where the CeCCs had more corrosion product than TCP samples. The CPDS results showed that when all passivations were broken down oxidation of the zinc into zinc compounds occurred. Impedance testing revealed that the coating systems with complex electrochemical phase

angle response curves had improved corrosion resistance in SST, but that resistance to polarization did not correlate to SST performance. The TCP based systems had a much more complex response, with several time constants seen in the Bode phase angle plot, compared to the CeCC. EIS was also done after SST and showed that all the passivations had a simple barrier response curve. Electrical contact resistance value correlated with the SST corrosion performance and electrochemical response where the coatings with the least amount of corrosion product had the lowest contact resistance. The TCP based coating systems had the lowest electrical resistances, making it a viable alternative to the CrCC system currently in use.

The intended journal for Paper II is *Transactions of the Institute of Metal Finishing.* The second paper characterized the microstructure and chemical composition of the coating systems before and after SST. The microstructures were compared using scanning electron microscopy (SEM). The microstructure of the developed corrosion products were vastly different from one another, although the thicknesses of the passivations were about the same. This showed that the morphology of the corrosion product that developed depended on the way the chemical composition of the passivations responded to corrosion. All coatings systems developed some corrosion, but TCP and one of the TCP variants exhibited very little corrosion. The chemical composition of the corrosion product was zinc hydroxycarbonate. The results from these experiments were compared to the results of paper 1 to determine that the TCP coatings would make a good alternative to chromate conversion coatings on γ-ZnNi.

1.3 IMPACT OF WORK

This work found that TCP and CeCC based passivations had very different responses on γ-ZnNi. TCPs were more active than CeCCs and produced more time constants on the Bode phase angle plot and peaked at higher frequency. The more complex electrochemical response correlated to less corrosion product during ASTM B117 testing. As zinc nickel alloys become a more popular choice for corrosion prevention to replace cadmium, this work can be used as a guideline for future work looking at other passivation alternatives to chromates.

2. LITERATURE REVIEW

2.1 ELECTROPLATED γ-ZINC NICKEL COATINGS

Zinc nickel coatings have been studied since the mid-1960s to improve corrosion resistance compared to nominally pure zinc coatings.[1] These coatings are formed by an anomalous codeposition process and were one of the first systems to use this method of deposition.[2] Zinc nickel coatings are used or have been proposed for use in many industries such as the automotive and aerospace industries.[3] Coatings containing 11 to 14 wt% nickel have improved corrosion resistance compared to electrodeposited zinc, with nearly a four-fold decrease in corrosion rate.[3, 4]

The zinc-nickel system has several single solid phases that are stable at room temperature (Figure 2-1). At room temperature, the face centered cubic nickel structure is stable up to ~27 at% Zn. The β_1 phase is a solid solution phase with the nominal composition of ZnNi. It has the AuCu-based structure and a composition range from 45.5 to 52 at% Zn. The γ phase, which has a composition range from 74.3 to 85 at% Zn, has the γ brass-based structure. The δ phase of zinc nickel is monoclinic and has a narrow range of stability at ~89 at% Zn. Finally, Ni is nearly insoluble in Zn, meaning that nearly pure Zn is the only other phase in the system.[5] For corrosion protection, the zinc-nickel alloy of interest is γ-phase ZnNi (γ-ZnNi) because of its mechanical properties, wear behavior, and corrosion resistance. This ZnNi phase has a yield strength of 260 MPa, elongation to failure of 0.7%, and a hardness of 2.6 to 3.9 GPa.[4] For comparison commercially rolled zinc has a lower tensile strength (up to ~190 MPa), an elongation of 40 to 60% and a hardness of 0.4 GPa.[6] Because γ-ZnNi is a candidate for replacement of Cd, the properties of Cd are a tensile strength of up to ~85 MPa, 50% elongation and a hardness of ~0.2 GPa.[7] Hence, γ-

ZnNi has improved strength and hardness compared to coatings that it may replace. Second, γ-ZnNi has enhanced wear resistance compared to cadmium and zinc coatings. After wear testing, the open circuit potential of the γ-ZnNi became electrochemically nobler and resistance to polarization (R_p) values increased. These responses were interpreted to indicate that dezincification during wear increased the relative amount of exposed nickel.[8] As shown in Figure 2-2 the increased R_p values for γ-ZnNi (Zn-Ni(2)) show that the coating is becoming more resistant to corrosion during wear compared to Zn, Cd, and other alloys.[8] The final reason for interest in γ-ZnNi is a lower average corrosion rate (Figure 2-3).[4] The corrosion resistance can be increased by incorporating ~12.5 wt% nickel to achieve the minimum corrosion rate, which is a four-fold reduction compared to a pure zinc.[4] Together, these properties make γ-ZnNi coatings a promising alternative to both Zn and Cd coatings.

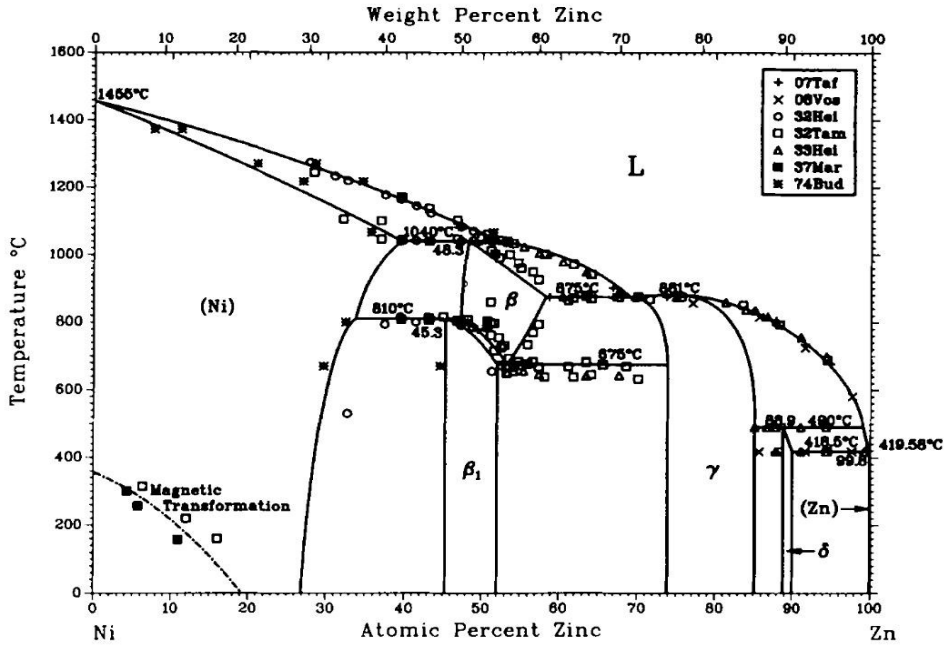

Figure 2-1: The Zn-Ni binary phase diagram.[5]

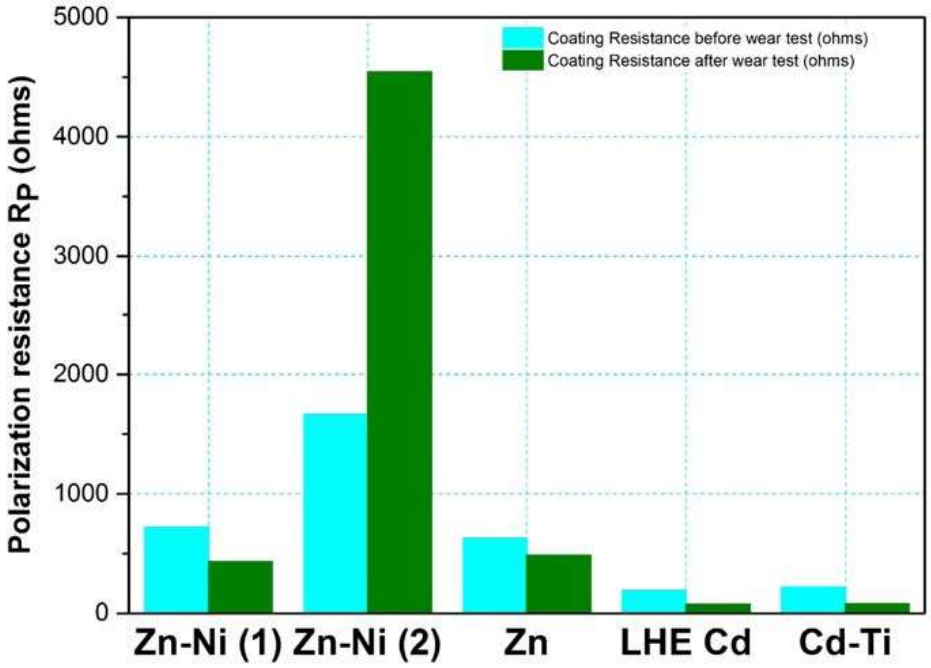

Figure 2-2: Resistance to polarization values before and after wear testing. Zn-Ni (1) was deposited at 48 mA/cm^2 (fine plate-like structure of γ-ZnNi), Zn-Ni (2) was deposited at 30 mA/cm^2 (large plate-like structure of γ-ZnNi), Zn coating was zinc, Cd coating was Cadmium, Cd-Ti coating was a solid solution of cadmium and Titanium.[8]

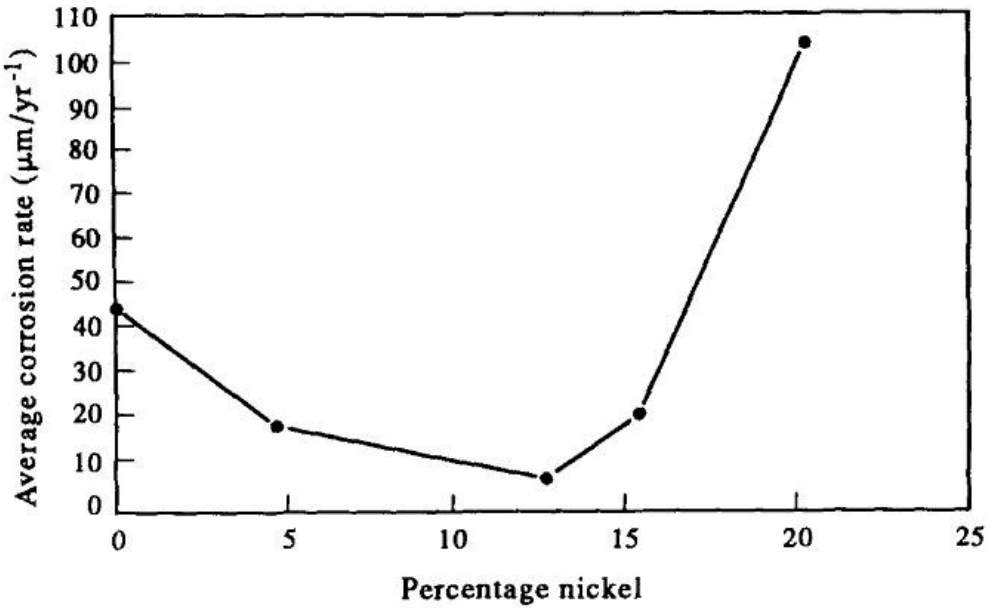

Figure 2-3: Average corrosion rate for ZnNi electrodeposits in 3.5 wt% NaCl solution, measured using a polarization pulse method.[4]

An anomalous codeposition method is used to deposit zinc-nickel coatings by either direct or pulsed current. [3, 9, 10] Physical vapor deposition can also be used to deposit ZnNi.[11] The commonly accepted theory for the mechanism for electrodeposition is that from a solution containing both Zn and Ni, zinc is deposited preferentially because it is more active than nickel.[3, 12] Then, as Zn starts to oxidize to $Zn(OH)_2$ due to a pH increase at the cathode, Ni deposition becomes favorable and will replace the $Zn(OH)_2$.[3, 12] Process parameters such as current density, temperature, additives, pH, and concentrations can be adjusted to control the ratio of Zn to Ni in coatings. These parameters also influence deposition kinetics, morphology, and the mechanical properties of ZnNi coating.[12] For example, metal ion concentration, temperature, and current density affect the microhardness as seen in (Figure 2-4).[13] An example of the current density affecting the morphology of the ZnNi is also seen in (Figure 2-5).[13] The deposition was performed at 40°C, with Ni^{2+}/Zn^{2+} ratio = 1 in the deposition solution. As the current density is increased, the size of the grains increased. Current density also affected the deposition time. If a thick coating with a fine grained microstructure is desired, then the deposition time must increase. Thus, deposition of ZnNi is a balance between multiple parameters.[13]

The electroplated γ-ZnNi has been studied as a potential replacement for toxic cadmium coatings.[14] Cadmium is a sacrificial coating on high strength steels and compatible with treatments that minimize hydrogen embrittlement of the underlying steel.[15] Hydrogen embrittlement weakens steel and is induced by water that is trapped in the coating or at coating/substrate interface that then reacts with the substrate and diffuses into it, making it brittle.[16, 17] γ-ZnNi can be compatible with low hydrogen embrittlement

(LHE) treatments since it can undergo a baking procedure to remove water.[18] The aerospace industry uses LHE γ-ZnNi as an effective cadmium replacement.[13]

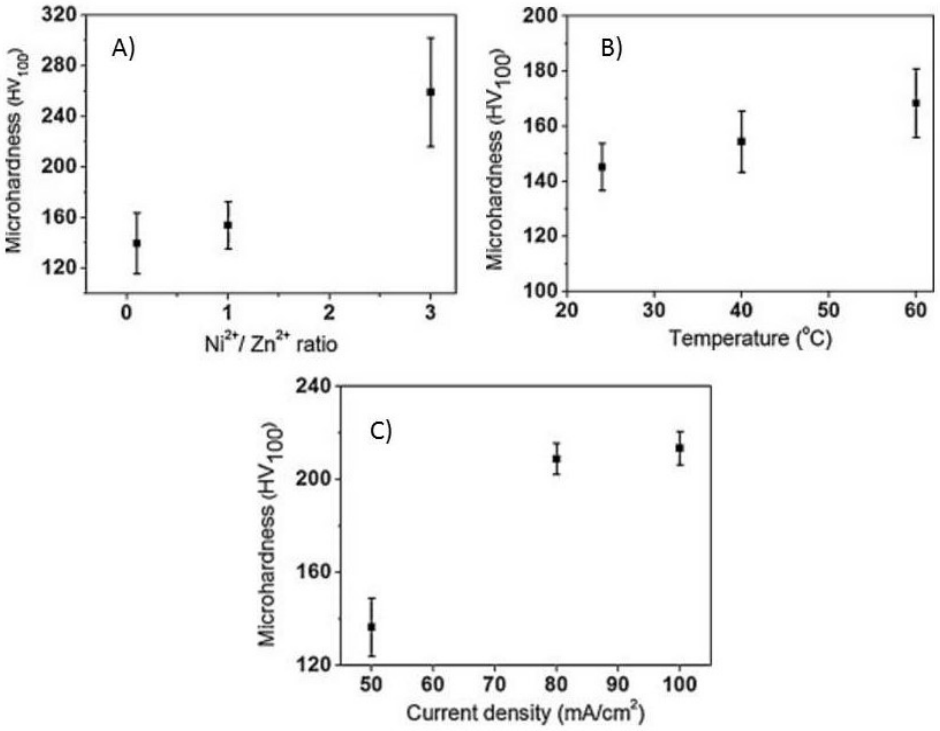

Figure 2-4: Microhardness vs; A) Ni to Zn ion concentration ratio, B) temperature, and C) current density.[13]

The corrosion properties of γ-ZnNi coatings are similar to cadmium; both coatings are sacrificial to steel in a corrosive environment and have relatively low corrosion rates.[19-21] The corrosion properties of γ-ZnNi have been well documented. Electrochemical Impedance Spectroscopy (EIS) has shown that γ-ZnNi coatings are a simple protective barrier with R_p values ranging from 600 to 1900 Ω/cm^2 depending on the deposition method.[10, 15] For comparison, cadmium has an R_p value of about 190 Ω/cm^2.[8] The corrosion potential (E_{Corr}) and corrosion current (I_{Corr}) vary depending on the grain size and composition of the γ-ZnNi coatings. [10] The reported E_{Corr} values range from ~-600 mV to ~-1100 mV with I_{Corr} values range from 20 to 50 μA/cm^2. [10, 11]

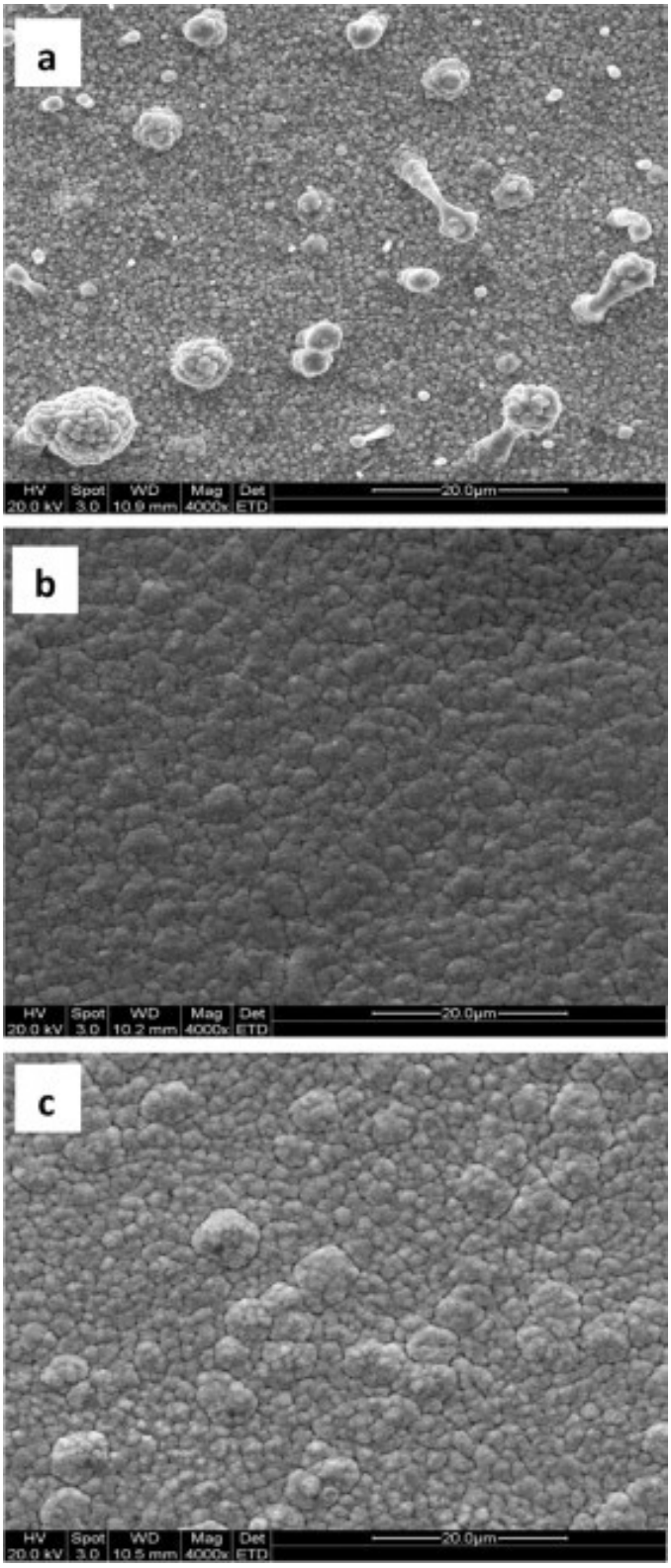

Figure 2-5: Surface morphology of ZnNi coatings by ESEM, electrodeposited at: (a) 50, (b) 80, and (c) 100 mA/cm^2.[13]

Kwon et al. studied the corrosion behavior of electroplated ZnNi with Ni content below 11 wt% and they concluded that corrosion resistance increased as the nickel content increased and was maximized at 10 wt% Ni approaching the γ-phase. [21, 22] Ganesan et al. studied electroplated ZnNi from 15 to 30 wt% Ni at the coating surface and found increasing the nickel content further in modulated ZnNi deposits to 30 wt% improved corrosion resistance in electrochemical tests; however, coatings with the lower 20 wt% nickel resisted corrosion for about 100 hours more than other compositions when tested in ASTM B117 salt spray.[23] They concluded that using γ-ZnNi with a surface containing 20 wt% Ni would be a possible alternative to just γ-ZnNi.[23] Typically the ZnNi coatings are Zn rich in at the surface, due to the anomalous codeposition method.[3] By increasing the Ni content at the surface, the corrosion rate will decrease due to a more positive (noble) potential. These studies helped to confirmed that the ideal range for Ni content is between 10 and 15 wt% Ni for use in corrosion based applications.[4]

2.2 PASSIVATION COATINGS

Passivation coatings are typically less than 500 nm thick oxide-based coatings that prevent substrates from reacting with external environments.[24-27] Passivations are composed of materials with low solubility and non-reactive to the external environment. These coatings are usually formed by chemical conversion of the substrate surface when an anodic half-reaction leads to dissolution of the substrate and then formation of the passivation by the cathodic half-reaction.[28-30] These reactions can be induced either by applying a current or by taking advantage of the electrochemical interaction between the substrate and the deposition solution. This review will cover three types of passivation

coatings: hexavalent chromate conversion coatings, trivalent chromium-based passivation coatings, and cerium-based passivation coatings.

2.2.1 Hexavalent Chromate Coatings. Hexavalent chromium coatings (CrCCs) have been widely used by the aerospace and other industries for corrosion protection. The CrCCs are composed of a matrix of complexes of trivalent chromium hydroxides, oxides and hydrates.[31, 32] Within the matrix, hexavalent chromium ions act as an active corrosion inhibitor while the matrix is an effective environmental barrier.[33] The hexavalent chromium ions have the ability to be released during corrosive attack followed by migration to the site of damage.[34] The chromate ions then oxidize, forming insoluble trivalent chromium complexes.[34] Kendig et al. found that the hexavalent chromium ions can absorb rapidly onto surfaces and then inhibit cathodic reactions occurring at Cu-containing aluminides in Al 2024-T3.[29] The ability of CrCCs to release from the coating matrix, migrate to the site of attack, and react to passivate the attack describes its ability to self-heal. For example, when corrosive attack leads to dissolution of the aluminum substrate (Reaction 1), CrCC coatings respond by releasing chromate ions that react to passivate the damaged area by Reaction 2. [35]:

$$2Al_{(s)} \rightarrow 2Al^{3+}_{(aq)} + 6e^{-} \quad (1)$$

$$Cr_2O^{2-}_{7\,(aq)} + 8H^{+}_{(aq)} + 6e^{-} \rightarrow 2Cr(OH)_{3(s)} + H_2O_{(l)} \quad (2)$$

This is one example of a possible reaction mechanism that could provide the self-healing behavior observed in CrCCs. The trivalent chromium hydroxide complexes are inert over a wide range of pH values, providing a stable coating.[29] While CrCCs provide excellent corrosion protection, hexavalent chromium ions are carcinogenic and dangerous

to the environment.[36] As a result, chromates are regulated by governments around the world.

2.2.2 Trivalent Chromium Coatings. Trivalent chromium-based passivations (TCPs) were developed to replace hexavalent chromium-based coatings. The passivations are usually between 90 and 250 nm thick depending on the processing parameters.[25, 26] Trivalent chromium passivations are commonly considered safe to both humans and the environment because they do not contain appreciable amounts of hexavalent chromium.[37] Passivations derived from trivalent chromium are a combination of oxide and hydroxide chromium species that provide an insoluble coating to mitigate corrosion, it is also common for the substrate to form hydroxide species that become a part of the passivation.[25, 38] The chemistry of these coatings varies depending on the concentration and additives in the deposition solution. For example, cobalt is a common additive in TCP deposition solutions and it also becomes part of the coating.[39] Trivalent chromium passivations have the reputation for performance that depends on an array of processing parameters including surface preparation such as cleaning, concentration of the deposition solution, and temperature of the deposition bath, as well as surface activation, deoxidizer type, and the anions in the deposition solution. [40] These parameters need to be optimized for each different substrate type to obtain consistent corrosion performance. [41]

A study by Gardner and Scharf compared TCP and CrCC coatings on zinc and zinc alloy substrates.[42] Both passivations performed similarly in ASTM B117 salt spray testing when TCP coatings were between 250 and 500 nm thick. The extra thickness was needed to reduce the chance of a defect compromising the coating since TCPs do not have self-healing capabilities. Interestingly, TCP coatings survived thermal shock at temperatures of

150˚C in contrast to CrCCs that developed severe cracking under similar conditions, which caused a loss of corrosion resistance. The poor performance of CrCCs was attributed to dehydration of hexavalent chromium compounds, which are required to enable self-healing. The TCP on the other hand survive elevated temperatures and maintained corrosion performance.[42]

Comparing coating morphologies, CrCCs have microcracks whereas TCP coatings do not.[42] Microcracking is caused by CrCCs being thicker than TCPs. However, cracking could also be from dehydration of the hexavalent chromium species.[42] Zhang et al. also observed etched zones that indicated that TCP deposition was influenced by the orientation of the underlying zinc grains. Also, Zhang et al. discussed the electrochemical mechanism thought to inhibit corrosion. Polarization experiments in aerated and de-aerated aqueous solutions of NaCl showed that corrosion of zinc was dependent on oxygen diffusion. These tests showed improved corrosion resistance in de-aerated solutions, which lead to the proposed mechanism for the protection of TCP whereby it inhibits diffusion of oxygen to the substrate.[26] This corrosion protection mechanism is also supported by other studies. [39, 43, 44]

2.2.3 Cerium-Based Passivation Coatings. The research and development of a cerium-based passivation coating (CeCC) was a direct response to the workplace regulations imposed on use of the hexavalent chromium, which is commonly used as a corrosion inhibitor. Cerium compounds are of interest due to their low toxicity.[45] The first reported use of a CeCC was by Hinton, Arnott and Ryan in 1986. They discovered that a cerium-based passivation was deposited on an aluminum 7075-T651 substrate from a solution containing either $CeCl_3$ or $Ce(NO_3)_3$ salts when current was applied to the

substrate. [27] These coatings initially took hundreds of hours to deposit, but the use of oxidizers, such as hydrogen peroxide, reduced deposition time to just a few minutes.[27, 28, 46] The substrate used, surface preparation of the substrate, chemistry of the deposition solution, and post-treatment of the passivation impact the quality, thickness and corrosion performance of CeCCs.

Surface preparation prior to deposition of cerium-based passivations usually includes degreasing and etching steps. Degreasing removes any organic residue that is adhered to the substrate surface. The type of solution, temperature, agitation, and duration of cleaning of the substrate can all impact the condition of the passivation and these parameters are dependent on the substrate used. Typically an alkaline solution held at 55˚C for 5 min is used to degrease the surface.[47-50] Etching removes some of oxide layer on the surface of the substrate. Again, the processing parameters such as acid/base type, duration, temperature, and agitation can all have an effect on the condition of the passivation.[51] For example, the use of a 1 wt% sulfuric acid solution was able to activate the surface of Al 2024-T3 alloy 40 times more quickly than with just the use of an alkaline cleaner.[51] The type of substrate used determines many of the surface preparations needed.

The chemistry of the deposition solution also impacts the passivation. Additives such as an organic gelatin can produce a smoother textured passivation, which helps to increase the quality and performance.[50] Specifically for cerium-based passivations, gelatin additions stabilize the gas bubbles that are generated on the substrate surface during deposition.[50] Without the gelatin the deposition occur quickly and produce cracks.[50] The amount of hydrogen peroxide also affects the uniformity of the passivation, its thickness across the substrate, internal stress, and adhesion between the substrate and passivation.

Peroxide content affects deposition rate. Higher rates lead to areas of varying thicknesses because of differences in chemical composition across the substrate. The varying thicknesses of the passivation can lead to internal stresses and cracks which can affect the corrosion performance. [28, 46] Controlling the rate of deposition with use of additives can help to produce a better quality passivation.

Post-treatment, also known as sealing, converts the as-deposited cerium(IV) oxide hydrate to cerium(III) phosphate by exposure to a bath of a phosphate salt.[48, 49] Cerium(III) phosphate has a lower solubility than that of the oxide making for a better performing passivation.[48-50] Processing parameters such as type of phosphate salt used, temperature, and duration of immersion, can also impact the condition of the cerium-based passivation.[48, 49] Post-treatments have been able to increase the impedance of the cerium-based passivations in EIS studies by several factors (Figure 2-6). [49] The post-treatments used an aqueous solution with 2.5 wt% $NH_4H_2PO_4$ at 85˚C.[49] The use of a post-treatment can be an effective process to increase the corrosion performance of cerium-based passivations.

Spontaneous deposition of cerium-based passivations relies on electrochemical redox reactions.[47, 52] Deposition starts with the oxidation of the substrate. For this example, zinc dissolves by Reaction 3 with simultaneous reduction of oxygen and water by Reaction 4, which produces OH^- species that promote formation of the cerium deposition by an increase in local pH. As shown by Reactions 5 and 6, intermediate complexes that form during deposition rely on OH^- species both to form and to react to the final product of $CeO_2 \bullet 2H_2O$ by Reaction 7. The presence of hydrogen peroxide increases the rate of

deposition by generating OH^- species (Reaction 8), which increases the local pH near the substrate surface more quickly, leading to more rapid deposition.[47, 52]

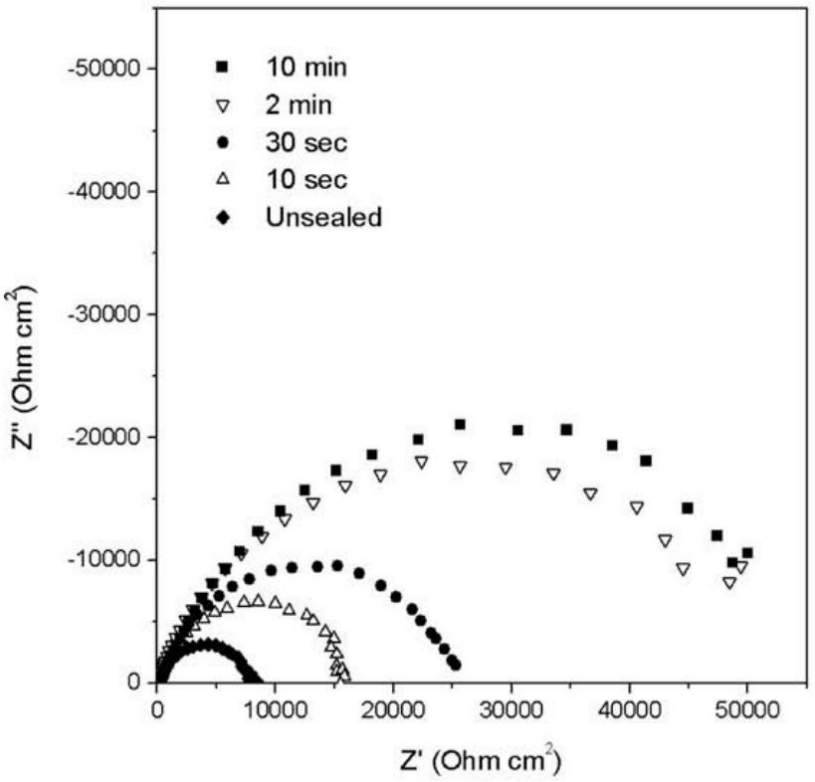

Figure 2-6: Effect of post-treatment as function of time in electrochemical impedance spectroscopy.

$$Zn_{(s)} \rightarrow Zn^{2+}_{(aq)} + 2e^- \tag{3}$$

$$O_{2(g)} + 2H_2O_{(l)} + 4e^- \rightarrow 4OH^-_{(aq)} \tag{4}$$

$$Ce^{3+}_{(aq)} + OH^-_{(aq)} + \tfrac{3}{2} H_2O_{(l)} \rightarrow Ce(OH)(OOH)^{2+}_{(aq)} \tag{5}$$

$$Ce(OH)(OOH)^{2+}_{(aq)} + 2OH^-_{(aq)} \rightarrow Ce(OH)_3(OOH)_{(s)} \tag{6}$$

$$Ce(OH)_3(OOH)_{(s)} \rightarrow CeO_2 \bullet 2H_2O_{(s)} + \tfrac{1}{2} O_{2(g)} \tag{7}$$

$$H_2O_{2(aq)} + 2e^- \rightarrow 2OH^-_{(aq)} \tag{8}$$

Cerium-based passivations have been produced on different substrate systems including aluminum alloys 2024-T3 and 7075-T6, magnesium alloys AZ31 and AZ91, stainless steel, zinc and δ-ZnNi.[46, 53-59] These cerium-based passivations inhibit corrosion by retarding the transport of oxygen to the substrate surface, which prevents the cathodic half-reaction from occurring. Unlike CrCCs, the CeCCs do not exhibit self-healing due to limited solubility of cerium species above a pH of around 2.[60] Even though CeCCs do not show self-healing, they are a promising alternative for CrCCs because they are able impede the diffusion oxygen to the substrate which can lead to corrosion.

2.3 ELECTRICAL CONNECTORS

Electrical connectors for U.S. military applications must meet stringent regulations.[61] These connectors must be resistant to corrosive environments, maintain their electrical conductivity at all times, and have an operating temperature range of -65˚C to +200˚C.[61] Because of this, a number of different classes of connectors have been defined and each one requires a unique combination of materials to achieve the desired properties.[61] The most significant standards that electrical connectors must meet include polarization of the connector shells, pin to pin mating, interchangeability, thermal shock and cycling, plating adhesion, air leakage, corrosion resistance, and contact resistance.[61] The main parts of electrical connectors are a shell, pins, insulator, and plugs. The shell is exposed to the environment and is usually made of aluminum or steel that is coated in nickel, gold, cadmium or other corrosion resistant materials, which may also have a passivation coating. Pins are usually copper plated with gold, but the pins can also be made from steel that is plated with cadmium and then passivated with a CrCC. The same materials are also used for connector plugs. The insulator is usually made of a dielectric material or a glass if the

connector is hermetically sealed. Figure 2-7 shows an example of a military grade electrical connector.[61] The Department of Defense is interested in replacing the cadmium used in these electrical connectors due to the toxicity of the metal. However, this has been a challenge due to many desirable properties of cadmium, which include low hydrogen embrittlement, galvanic compatibility, electrical conductivity and corrosion resistance.[61, 62] They have designated several different possible candidates to replace cadmium in these system, these include: Ni-fluorocarbon Polytetraflouroethelyne, ZnNi, and pure Al.[63]

Figure 2-7: Military grade electrical connector.[64]

2.4 CONTACT RESISTANCE

Electrical contact resistance is an important property for many applications in electrical devices, such as circuit breakers, relays, and connectors.[65] Electrical contact resistance is the resistance of a surface when in contact with another surface. This is important because many highly conductive metals develop an insulating oxide thin film on the surface when introduced to the atmosphere, and it is this film that can impede the flow of electrons, increasing the electrical contact resistance. Preventing the degradation of electrical performance is important, so a coating is used to maintain the desired contact resistance. These coatings are usually a nobler metal or a passivation coating. The passivation coating, which is usually oxide based, is also an insulator, but thin coatings

allow electrons to tunnel through the coating, making the coating electrically conductive.[65] Surface roughness also plays an important role in the measurement of contact resistance, Figure 2-8 shows how a global measurement is affected by the surface roughness.[65]

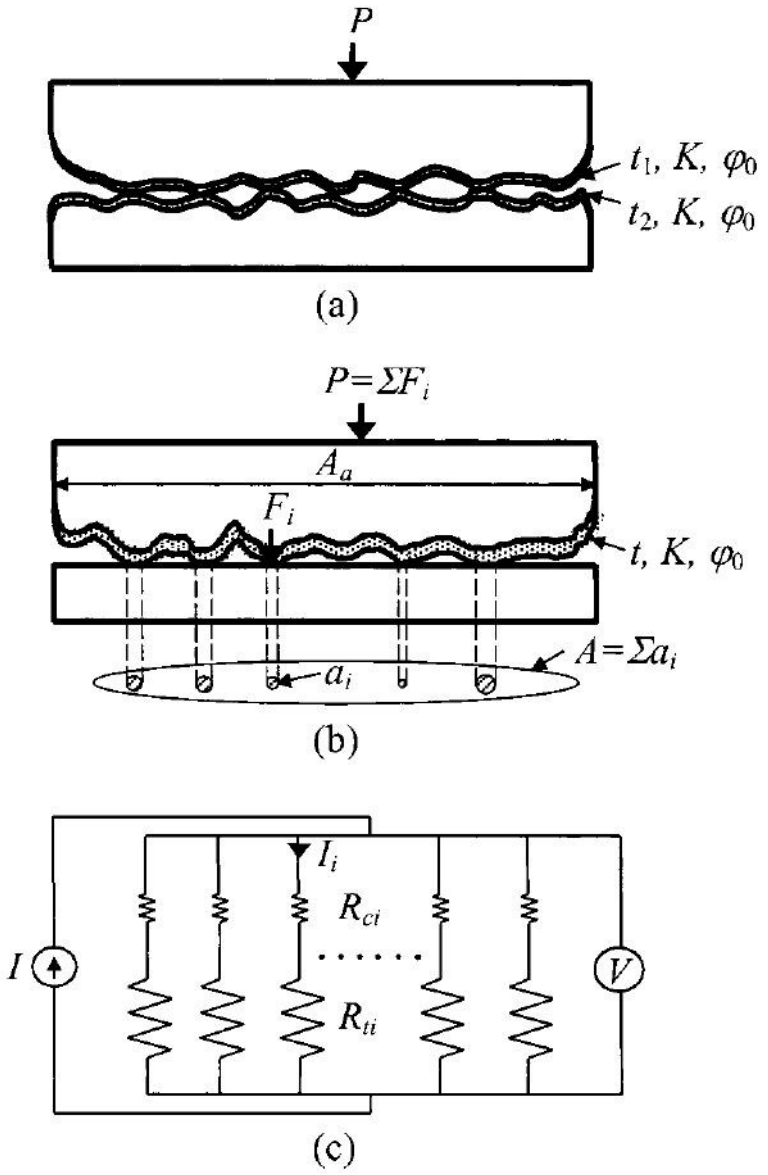

Figure 2-8: A) two rough surfaces in contact with a coating separating the bulk material, B) local contacts contributing to the resistance, C) electrical circuit model for the contact resistance.[65]

The contact resistance becomes a summation of the local resistances, at the peaks of the surface, in parallel with one another over the area being measured.[65] The actual value for contact resistance cannot be directly determined without knowing the area in contact. Control of the surface degradation and surface roughness are important for the control of the electrical contact resistance and are needed to be considered when an application needs a specific contact resistance.

2.4.1 Present Testing Method. Military specifications for electrical connectors list maximum contact resistance values and describe testing methods. The standard test method for connectors with surface passivations uses an applied pressure of 200 psi with the requirement that electrical resistance should not be greater than 5 $m\Omega/in^2$ for as-deposited coatings and not be greater than 10 $m\Omega/in^2$ after corrosion in ASTM B117 salt spray testing.[66] One study found standard deviations ranging from 19% to 47% of the average value for this method.[67] Contact resistance values can be affected by surface roughness as the electrode will only make contact at the peaks of the surface.[65] The inaccuracies from these issues and others have made it desirable to produce an alternative method to the current method.

2.4.2 Alternative Testing Method. Alternative methods to test contactresistance may offer better reproducibility. One alternative method is based on a probe with four conductor lines with width and spacing that depend on the thickness of the coating being measured (Figure 2-9).[68] Conductor lines are connected to a multimeter in a four-probe terminal resistance mode. The current probes are attached to the outside lines and the voltage probes are attached to the inside probes.[68] By measuring the voltage drop as the current travels from the positive current probe to the negative current probe, resistance can

be calculated.[69] The spacing of the probe lines affects the depth that current travels into the substrate. If line spacing is larger than the coating thickness, the current should travel through the coating, into the substrate, and then back out through the coating. This current path could be advantageous or a undesirable, depending on the measurement. When the line spacing is smaller than the coating thickness, current is confined to the coating, measuring just the resistance of the coating (Figure 2-10)[69] This method is a non-destructive method because it requires less applied pressure and a smaller area needed compared to the conventional contact resistance measurement used for military conversion coatings. This method reduces the effect of surface roughness on the measurement because the resistance value is being taken at a much smaller scale. Another application for this method is resistance mapping of surfaces, which could be used to probe quality and uniformity of surface passivations.[68]

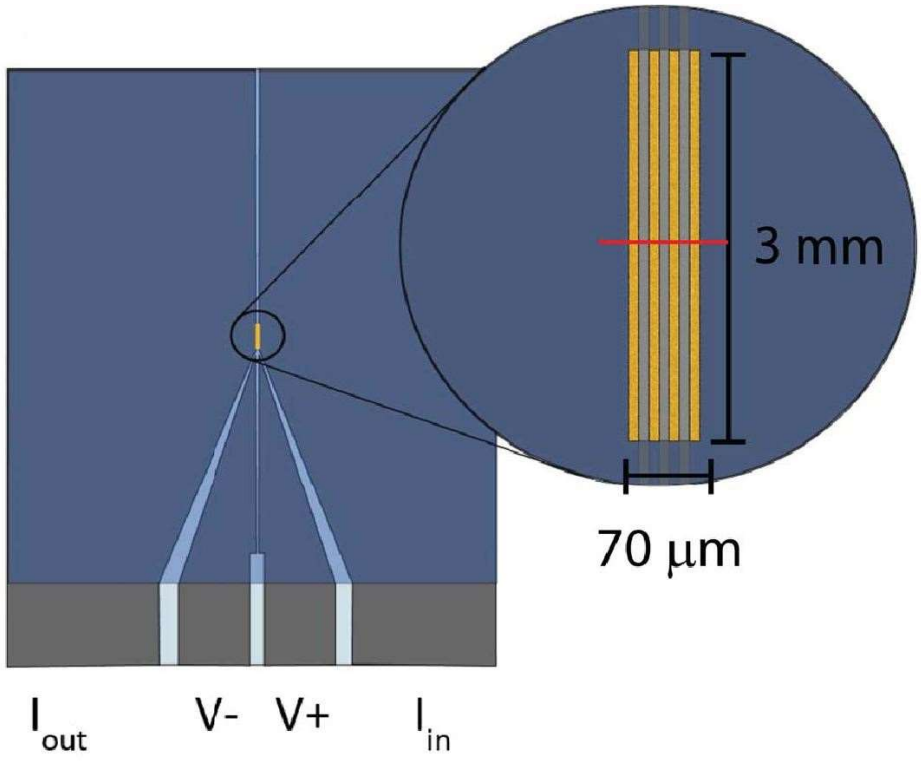

Figure 2-9: Example of a 4 line micro-probe.[68]

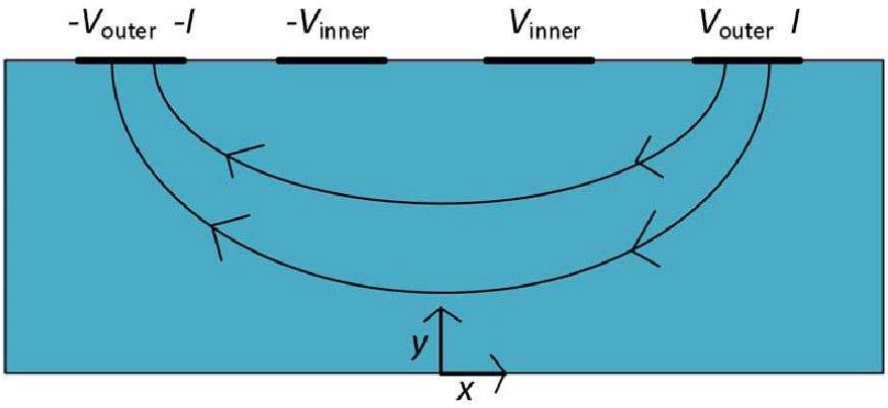

Figure 2-10: Example of current flow through the material.[69]

PAPER

I. CORROSION BEHAVIOR AND CONTACT RESISTANCE OF ELECTROPLATED γ-ZnNi WITH PASSIVATION LAYERS

S. M. Volz, J. B. Claypool, M. J. O'Keefe, W. G. Fahrenholtz

Materials Research Center, Department of Materials Science and Engineering,

Missouri University of Science and Technology, Rolla, MO 65401, USA

ABSTRACT

Corrosion behavior, electrochemical response, and contact resistance were examined for cerium-based conversion coatings and trivalent chromium passivations on electroplated γ-ZnNi on steel substrates. These passivations were compared to hexavalent chromate conversion coating. The electrochemical response was investigated using electrochemical impedance spectroscopy and cyclic potentiodynamic scans. The corrosion response of the passivations was studied using ASTM B117. The electrochemical testing was able to model the corrosion response by the use of equivalent circuit models. Cyclic potentiodynamic scan tests revealed a self-healing behavior between the γ-ZnNi and passivations. Trivalent chromium passivations and chromate coating had the lowest corrosion current between 46 and 57 $\mu A/cm^2$. Electrochemical impedance spectroscopy measurements demonstrated different response behavior between the type of passivation. The contact resistance of trivalent chromium passivations had the lowest values at 1 $m\Omega/cm^2$.

Introduction

Currently, the combination of an electroplated cadmium coating and a hexavalent chromium-based conversion coating (CrCC) provides corrosion protection used in Department of Defense (DoD) electrical system components.[1] This system meets the a DoD contact resistance specification with an as-deposited value that is <0.8 $m\Omega/cm^2$ (5 $m\Omega/in^2$) and a value <1.6 $m\Omega/cm^2$ (10 $m\Omega/in^2$) after exposure to a saline corrosive environment.[2]

Cadmium and chromates are toxic to both humans and the environment. Cadmium can lead to lung cancer and kidney degradation if inhaled.[3] Hexavalent chromium is very mobile in humans and other animals; it also is reactive with the biochemical oxidation mediators making it carcinogenic.[4] The toxicity and other adverse environmental effects have led to the regulations and have motivated the search for replacements. For example, OSHA 1910.1026, which limits the air concentration to 0.5 $\mu g/m^3$ of hexavalent chromium, led to the search for CrCC replacements.[5]

Low hydrogen embrittlement (LHE) alkaline γ-ZnNi (γ-ZnNi) is a potential replacement for cadmium. Because of several beneficial properties, γ-ZnNi has been approved for other aerospace applications. The alloy is sacrificial to steel in a corrosive environment, has a relatively low corrosion rate, and is compatible with low hydrogen embrittlement treatments.[6-8] Unlike cadmium, which is toxic, γ-ZnNi is environmentally benign. To maintain a low contact resistance, γ-ZnNi requires a passivation coating to mitigate the formation of corrosion products.[9] Currently, CrCCs are the only approved passivation for use with γ-ZnNi, and no other commercial non-CrCC passivations are currently approved for γ-ZnNi because they cannot consistently provide contact resistance

values that meet DoD specifications.[2] The goal of this research is to study the alternative passivations as potential replacements for CrCCs on γ-ZnNi coatings.

The CrCCs provide a trivalent chromium oxide-based barrier on metal surfaces and also contain hexavalent chromium species that can be released and transported to damaged sites on the surface.[4, 10] The hexavalent chromium species can be reduced to form trivalent chromium hydroxides and other complexes that inhibit corrosion.[11] The ability of CrCCs to self-heal results in a better corrosion response compared to other coating systems. Unfortunately, due to its health and environmental risks, alternatives to chromate passivations are needed.

Cerium-based passivations consisting of cerium oxides and/or phosphates have been used as a corrosion barrier due to their low solubility over a wide pH range.[11] Cerium compounds have also been accepted as an environmentally benign alternative, having only low to moderate toxicity when tested in animals.[12] The low solubility and the environmentally friendly nature of cerium-based passivations makes them potential alternatives to CrCCs. Cerium-based conversion coatings (CeCCs) have been deposited on several different metal substrates including aluminum alloys, magnesium alloys, and stainless steel.[13-17] These passivations can be deposited by spontaneous or electrolytic means from solutions of chloride or nitrate cerium salts in either an aqueous or organic solvent solutions.[13-17] These passivations consist of an insoluble coating of Ce^{4+} and Ce^{3+} complexes such as $CePO_4 \cdot H_2O$.[13-17] Hosseini et al. observed that CeCCs derived from $Ce(NO)_3$ treatments inhibited the transport of O_2 to the metal substrate thereby stopping the cathodic half-reaction.[18, 19] It was also noted in this study that δ-ZnNi with CeCCs were found to have comparable corrosion protection properties to that of CrCCs.[19] Joshi et al.

hypothesized that at low pH levels around 2 and below the CeCCs could have self-healing abilities, like CrCCs, but at pH levels above 2 the self-healing effects would be negligible, due to the low solubility of the cerium species.[11, 20] Most applications for the passivation are in neutral to basic environments, such as seawater, which has a pH of around 8. [21] The higher pH prevents the CeCCs from self-healing, but that are still able to provide an effective barrier to corrosion. The CeCCs are a candidates as a replacements for CrCCs because they are environmental friendly, have low solubility over a wide pH range, and are able to passivate many different metals.

Trivalent chromium-based passivations (TCP) have also been studied as potential CrCC alternatives. Studies have found that trivalent chromium-based passivations on zinc have good corrosion resistant properties.[22-24] However, due to a lack of self-healing ability, TCP coatings cannot provide a good of corrosion performance as CrCCs.[25] The TCP coatings contain predominantly trivalent chromium oxides and hydroxide hydrates, the structure and properties of which can be altered with different anions in the deposition solution.[26] These compounds are stable and have low solubility in corrosive environments, thus providing a barrier to corrosion.[27] The barrier effect of TCPs inhibits corrosion by reducing the diffusion of oxygen to the metal substrate. This, in turn, can hinder the cathodic half-reaction during corrosion.[23, 28, 29] TCP coatings have low toxicity since they contain Cr(III) species.

The purpose of this research was to evaluate environmentally friendly passivations for ZnNi coatings that are able to provide adequate corrosion protection, while maintaining low contact resistance.

Procedure

Six different passivations were evaluated. All passivations were deposited on electroplated with LHE γ-ZnNi (IZ-C17+, Dipsol of America, Livonia, MI) that had been deposited on steel substrates. The γ-ZnNi coatings contained about 14 wt% nickel and were just over 10 μm thick. A commercially available TCP (IZ-264, Dipsol of America, Livonia, MI), an experimental cobalt-free TCP (Co-Free, from Dipsol) and an experimental modified cobalt-free TCP (Co-Free Mod, from Dipsol); and a commercially available CrCC passivation (IZ-258, Dipsol), were provided by the manufacturer already deposited on substrates with an LHE γ-ZnNi coating. Steel substrates electroplated with LHE γ-ZnNi were also provided by Dipsol for the deposition of CeCCs. Two types of CeCCs were produced, one from chloride-based salts (CeCC-Cl) and the other from nitrate-based salts (CeCC-N).

Cerium-based passivation deposition

The γ-ZnNi substrates were first wiped clean with ethanol on a laboratory wiper. Then the substrates were immersed in an alkaline cleaning solution (Turco 4215 NC-LT, Henkel) at 55˚C for 5 minutes to degrease the surface and then rinsed with deionized (DI) water. Next, the panels were immersed in an aqueous solution containing 0.037 mol/L HCl for surface activation. Immersion time was 30 seconds at room temperature and then panels were rinsed with DI water. The substrates went through either one of two deposition baths, one based on cerium chloride or a second based on cerium nitrate. The cerium chloride bath consisted of 4.2 wt% cerium chloride hexahydrate (Alfa Aesar, 99.9%, Ward Hill, MA), 4.2 wt% (Fisher Scientific, 34-37% technical grade, Fair Lawn, MA) hydrogen peroxide solution and 0.3 wt% (Rousselot DSF, Dubuque, IA) gelatin in an aqueous

solution that was adjusted to pH = 2 with HCl. The cerium nitrate bath consisted of 4.8 wt% cerium nitrate heptahydrate (Acros Organics, 99.5%, Geel, Belgium), 4.1 wt% (Fisher Scientific, 34-37% technical grade, Fair Lawn, MA) hydrogen peroxide and 0.3 wt% (Rousselot DSF, Dubuque, IA) gelatin in an aqueous solution that was adjusted to pH = 2 using HNO_3. The substrates were immersed in either bath for 2 minutes at room temperature. Post-treatment of the cerium passivations was done in a 2.5 wt% sodium phosphate monobasic dihydrate (Fisher Scientific, 99.8%, Fair Lawn, NJ) solution at 85˚C of 5 minutes and then rinsed with DI water. The panels were allowed to air dry for at least 24 hours before testing.

Corrosive environment exposure

Corrosion behavior was evaluated in salt spray testing (Q-fog, Q-Panel Lab products) performed according to ASTM B117. A 5 wt% sodium chloride solution was used, as specified in the standard. The testing was performed on each of the passivations for 1000 hours. The passivations were visually evaluated at 100 hour intervals.

Contact resistance

A device was built to test contact resistance by the method specified in MIL-DTL-81706. The device used two solid copper electrodes one of which was a 6.45 cm^2 area that made contact with the passivation covered side of the sample. The second electrode was slightly bigger and made contact with the exposed metal side of the sample. A pressure of ~1.4 MPa was applied to the electrode. A multimeter measured the contact resistance in four-terminal resistance mode. Five measurements were taken from different areas on each panel to determine the reported values.

Electrochemical analysis

A flat cell (model K0235, Princeton Applied Research), with a saturated calomel electrode (SCE) electrode, was used for all the electrochemical analysis. The electrolyte was an aqueous solution containing 0.6 M ammonium sulfate and 0.6 M sodium chloride. Experiments were conducted using a potentiostat (EG&G Princeton Applied Research, Model 273A) and a frequency response analyzer (Solartron Instruments, SI 1255). The software used was for data collection and analysis was from Scribner Associates, Inc. Zplot and Zview software packages were used for EIS data collection and analysis, respectively. Corrware and CorrView software packages were used for CPDS data collection and analysis, respectively. Reported results from electrochemical analyses were the average of four different measurements performed at different locations on each specimen.Prior to analysis, the passivations were allowed to reach their open circuit potential (OCP) over a time period of 2000 seconds before starting electrochemical impedance spectroscopy (EIS). EIS was performed over a frequency range of 10^{-2} to 10^{5} Hz with AC amplitude of 10 mV. After EIS, cyclic potentiodynamic scans (CPDS) were conducted at a 1.5 mV/s scan rate and ran from -0.4 V from OCP to OCP for the cathodic sweep and from OCP to -0.6 V from the OCP for the anodic sweep. The maximum overpotential reached during the scan was at 0.7 V from OCP.

Results and discussion

As-deposited passivations

Passivation coatings on γ-ZnNi generally all had a yellow or gray coloring to them (Figure 1). Some regions had different coloring, which could indicate different passivation thicknesses across the surface of the panel. For CeCC-Cl, the passivation had a slightly

darker gold color on the left of the panel but was more pale yellow on the right. This could also indicate that the passivation is slightly thicker on the left. Other passivations that possibly had varying thicknesses were CeCC-N and CrCC, which could indicate that these regions also had different properties. For example, contact resistance is directly dependent on the thickness of the passivation. The thickness of the passivations can also impact the corrosion performance. If the passivation is too thin, the passivation may not be able to provide a barrier to corrosion or may not cover the entire surface of the substrate. If the passivation is too thick, the passivation could crack and expose the more reactive substrate.[30] Passivation thickness cannot be directly determined by color; however, color variations across the surfaces of passivations can provide a qualitative explanation for the variance in measurements. The electrical contact resistance of Co-Free and Co-Free Mod passivations help to support this, as visually the passivations have a very even gray color across the panel surface and these passivations have the lowest deviation in the contact resistance measurements (Table 1). In contrast, the passivations noticeable color change across the surface, such as CeCC-Cl, CeCC-N, and CrCC, had variances in the electrical contact resistance of 20% to 42%. Variations in color across the surface of passivations are probably due to the variations in processing parameters. For example, CeCC passivations rely on an increase in the local pH level in order for the passivation to deposit. If variations in surface preparation result in differences in surface chemistry, then areas of different pH would develop across the surface during deposition, which would impact the thickness of the deposit in those areas. This issue could arise because of the panel orientation. For example, if the panel were suspended vertically in the deposition solution, bubbles that form near the top of the panel during deposition could change the local

chemistry in that area and thereby affect the passivation thickness. Possible ways to fix this issue would be to either agitate the solution during deposition to insure the chemistry across the panel is consistent or to electrodeposit the passivations. These changes to the processing could help with variance issues and should be considered in future work.

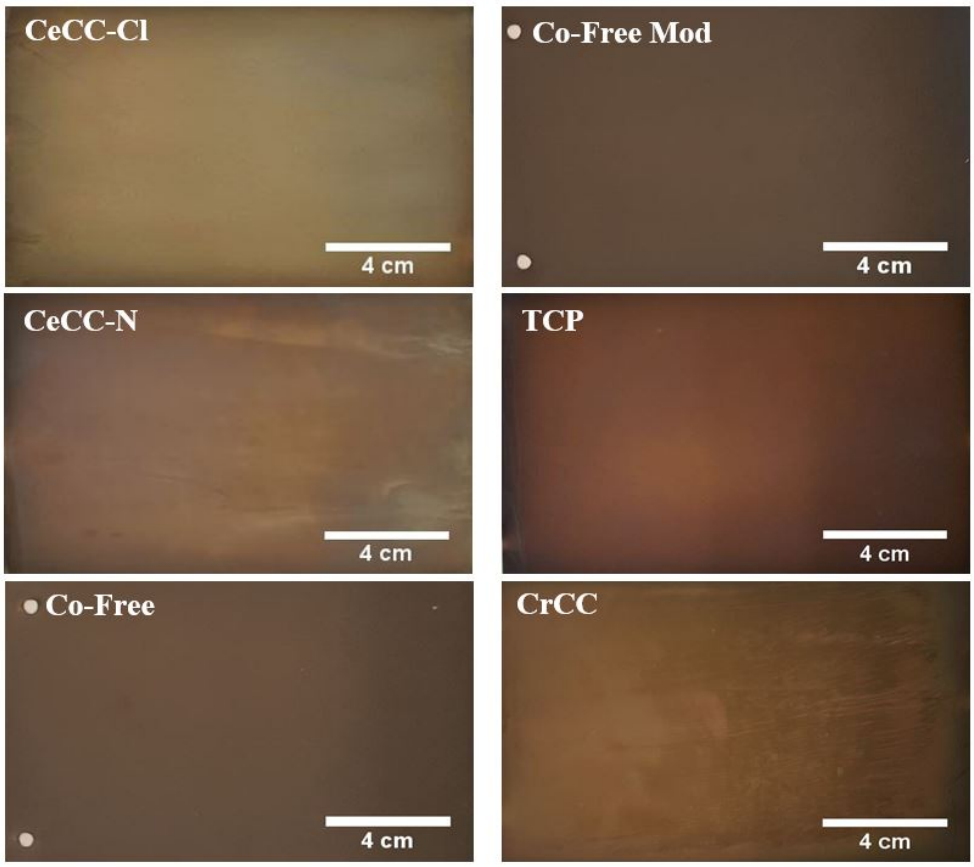

Figure 1: Optical images of as-deposited passivation coatings on γ-ZnNi substrates.

The Co-Free and Co-Free Mod passivations had the lowest contact resistances and had least variation between the measurements (Table 1). This could be attributed to coating uniformity as discussed above. The other passivations had variations ranging from about 20% to 40% in the measured contact resistances. The Co-Free Mod coating had the lowest resistance at 0.1 $m\Omega/cm^2$ with no variance based on the level of precision of the measurement. The TCP coating had a higher resistance at 0.8 $m\Omega/cm^2$, but was still

acceptable based on the requirement of contact resistance of 0.8 mΩ/cm^2 or lower in the DoD standard [2]. All of the passivation coatings, except CeCC-Cl, fell between those of Co-Free Mod and TCP.

Factors that could have affected the contact resistance other than composition of the passivation material are passivation thickness and surface roughness. The surface roughness is the same for all panels since the starting γ-ZnNi coatings were all nominally identical. Hence, the effect of surface roughness of the initial ZnNi surface on contact resistance of the passivations were assumed to be negligible. Thickness, on the other hand, varies among passivations. The thickness of the passivations was on the order of 100 nm, which can drastically effect the measured resistances. The thickness of the passivations are process dependent, as such a variety of parameters can affect the thickness. Specifically for cerium-based conversion coatings, parameters such as peroxide content, immersion time, and pH of deposition solution can all have an effect on the final passivation thickness. The contact resistance and the variation of the contact resistance across the panel are dependent on the control of these parameters.

Table 1: Contact Resistances of As-deposited Passivations

	mΩ/cm^2
CeCC-Cl	1.2 ± 0.5
CeCC-N	0.6 ± 0.2
Co-Free	0.2 ± <0.1
Co-Free Mod	0.1 ± 0.0
TCP	0.8 ± 0.1
CrCC	0.5 ± 0.1

CPDS results (Figure 2) showed that the shapes of the curves were similar for each of the different passivations. The corrosion potential of all the passivations fell between -650 mV to -860 mV. A secondary corrosion potential occurred at about -450 mV for all of the passivations. The passivations breakdown when a rapid increase in the observed potential occurs, exposing the underlying γ-ZnNi. Then, as the potential dropped, the γ-ZnNi oxidized to a ZnO complex, producing the secondary corrosion potential. The potential is more positive than the initial corrosion potential meaning that the new coating of a oxidized zinc compound is more electrochemically noble than the initial passivation, making the coating systems self-healing whereby failure of the surface passivation exposed the underlying γ-ZnNi, which then reacted to form a Zn-based protective layer.

The values for the corrosion potential (E_o), corrosion current (I_o), and polarization resistance (R_p) are displayed in Table 2. The lowest I_o values belonged to CrCC, CeCC-N TCP coatings, which indicated that these three coatings had lower corrosion rates compared to the other passivations. These passivations also had the highest polarization resistance (R_p) values, which indicated that they were more resistant to corrosion. In contrast to CrCC and TCP, the Co-Free and Co-Free Mod passivations were the most active with the lowest E_o values at -820 mV and -860mV, respectively. CrCC, CeCC-Cl, and CeCC-N had high E_o values around -650 mV and -670 mV making these passivations more noble. From these results, the CeCC-N, CrCC, and TCP passivations had higher resistances to corrosion with lower corrosion rates and higher resistances to polarization. The CrCC passivation had the lowest corrosion rate and highest R_p value, which made it the least susceptible to corrosion.

Table 2: CPDS Polarization Values of As-deposited Passivations

Coatings	I_o (mA/cm^2)	E_o (V)	R_P (Ω•cm^2)
CeCC-Cl	0.170 ± 0.10	-0.67 ± 0.01	166 ± 37
CeCC-N	0.056 ± 0.04	-0.67 ± 0.00	313 ± 42
Co-Free	0.064 ± 0.05	-0.86 ± 0.04	229 ± 80
Co-Free Mod	0.194 ± 0.07	-0.82 ± 0.01	148 ± 35
CrCC	0.046 ± 0.01	-0.65 ± 0.00	585 ± 126
TCP	0.057 ± 0.01	-0.72 ± 0.02	471 ± 98

The Bode plots for the cerium-based passivations (Figure 3, A) showed that they were a simple barrier to corrosion. Each coating had a single peak, which was at 2 Hz for CeCC-Cl and 6 Hz for CeCC-N. The single peaks indicated a single time dependence for the coating systems. The EIS data for the chromium-based passivations showed a more complex response on the Bode plot (Figure 3, B). For example, TCP had two peaks at about 1 Hz and 20 Hz. Likewise, CrCC had either 2 or 3 peaks at 1 Hz, 20 Hz and what also appears be a peak at 104 Hz. Co-Free had a peak at 1 Hz and a complex response at lower frequencies below 1 Hz. The Co-Free Mod passivation had a similar response as the Co-Free passivation, except for a peak at 40 Hz, with a complex response occurring at frequencies below 40 Hz. These multiple peaks and complex responses indicate multiple time dependencies contributing to the phase angle response, which implies that the passivations were more than just simple barriers to corrosion. The passivations, in this case, were providing either active or passive corrosion protection with what could be multiple layers, porous layers, or a combination of these contributing to the response. Bode plots were able to show distinct differences between CeCCs and chromium-based passivations on γ-ZnNi, with CeCCs being a passive barrier and chromium-based passivations providing active corrosion protection.

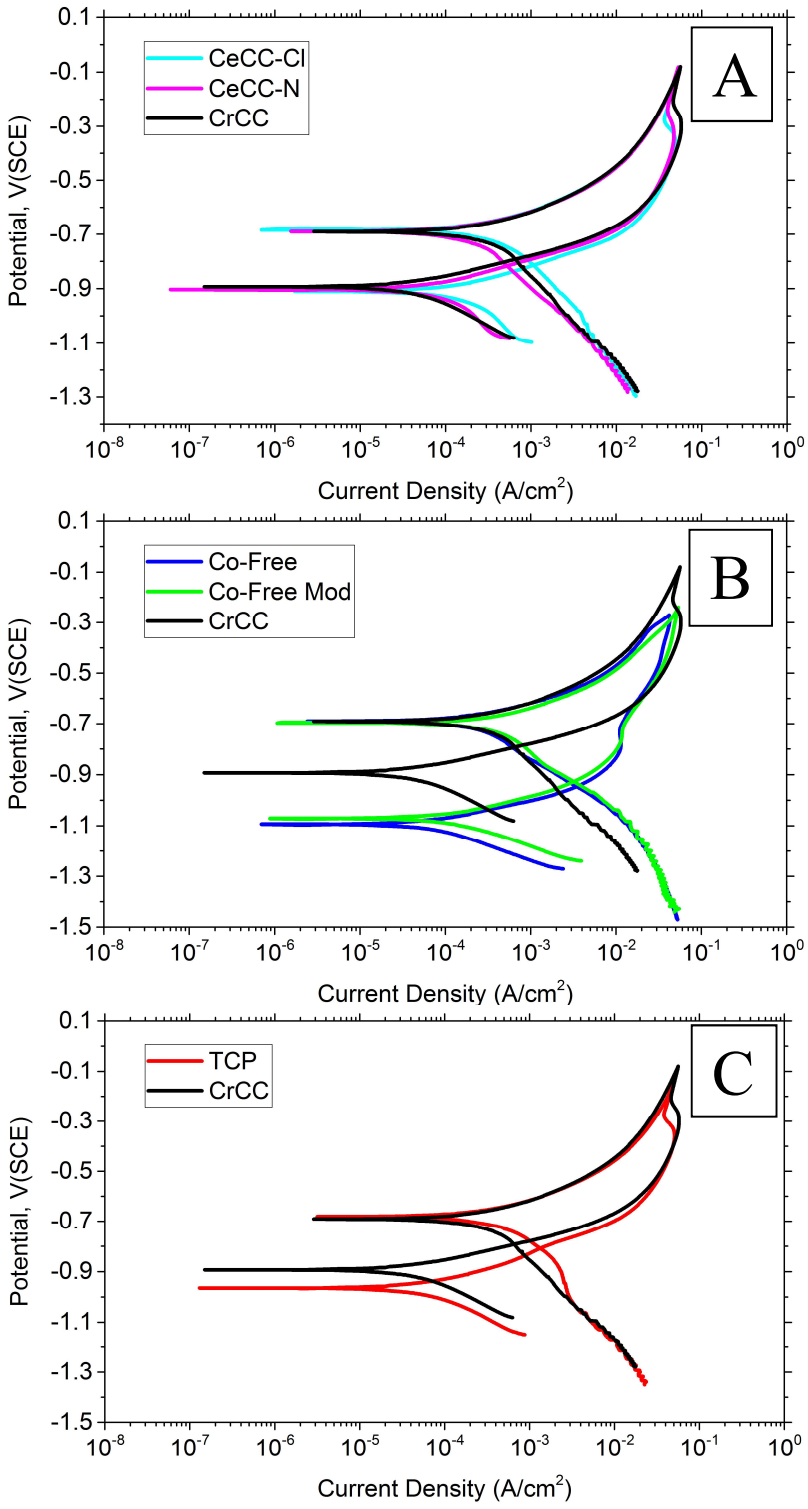

Figure 2: CPDS curves comparing; A) Cerium-based passivation coatings (CeCC-Cl, CeCC-N), B) Cobalt-Free trivalent chromium passivation coatings, and C) Trivalent chromium passivation to the hexavalent chromium conversion coating control.

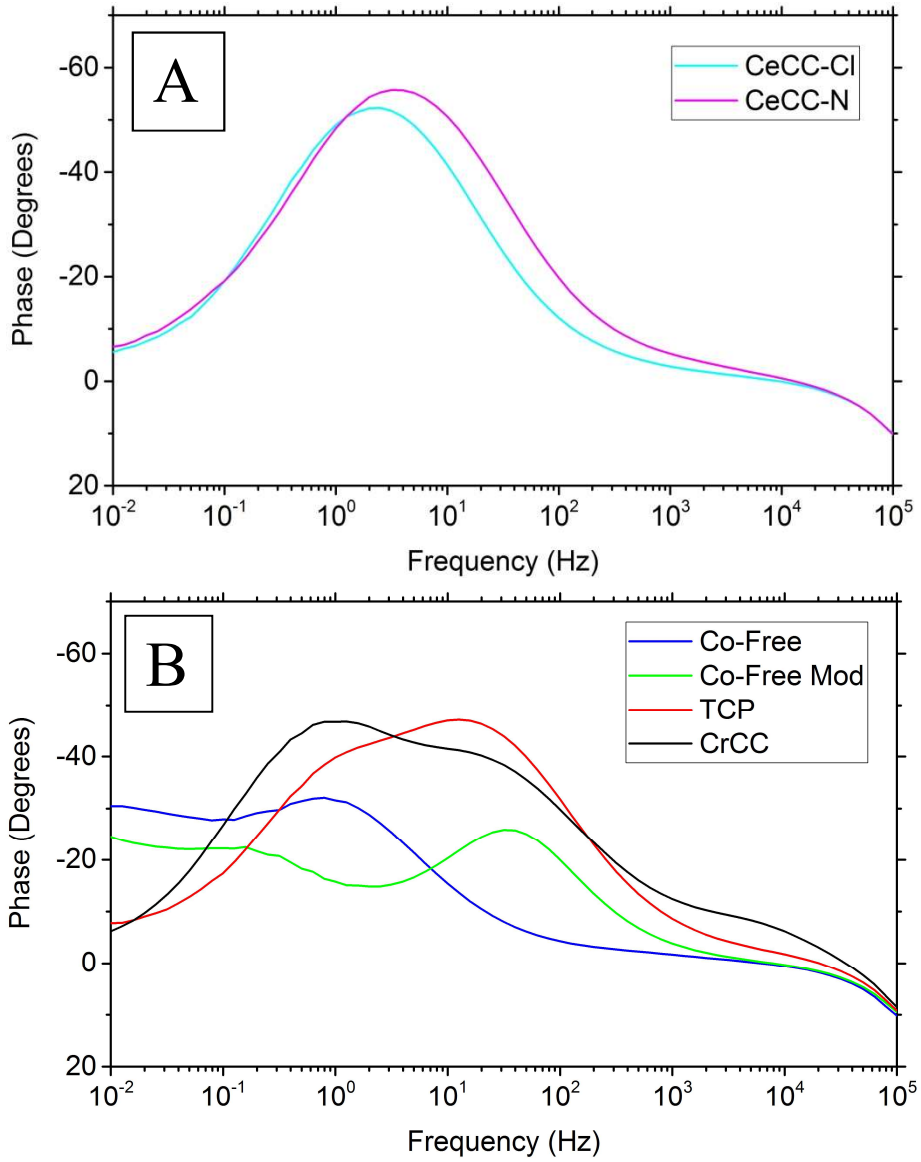

Figure 3: Bode plots: A) single time dependencies for the cerium-based passivations. B) Multiple time dependencies in the CrCC, TCP, Co-Free and Co-Free Mod passivations.

Nyquist plots for the passivated samples (Figure 4) show both of the CeCCs, TCP, and CrCC produced a semicircular response and these passivations had the largest impedance values, which were 200 Ω/cm^2 for CeCC-Cl, 300 Ω/cm^2 for CeCC-N, 350 Ω/cm^2 for TCP, and 500 Ω/cm^2 for CrCC. These responses are indicative of passivations with uniform surfaces. The most active passivations, Co-Free and Co-Free Mod, had the

smallest impedance values and had different responses compared to the rest of the passivations. These passivations had the smallest impedance magnitudes and the responses

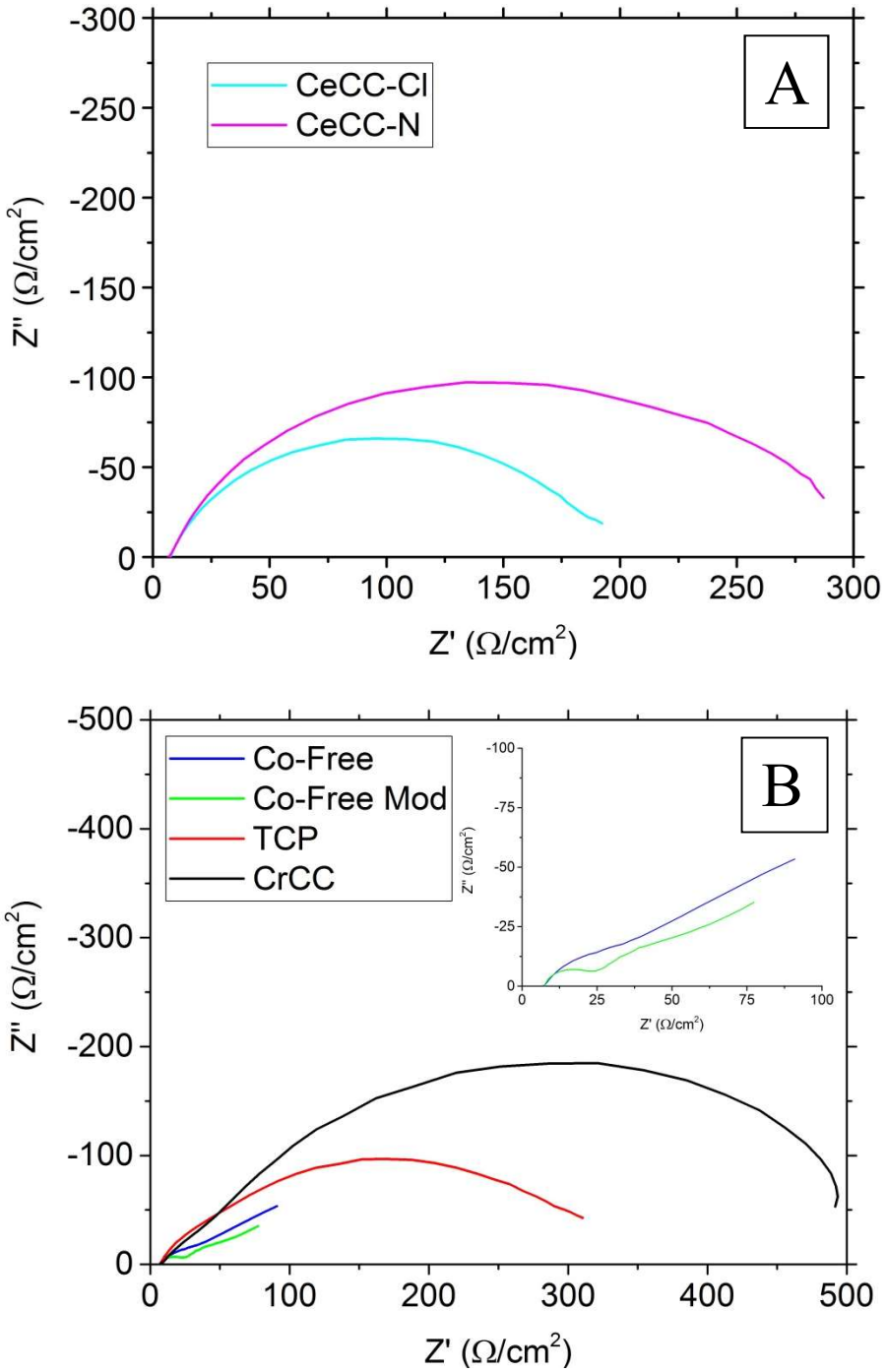

Figure 4: A) Nyquist plot for the as-deposited cerium-based passivations. B) Nyquist plot of the as-deposited chromium-based passivations.

had a linear section at low frequencies. This linear section is indicative of Warburg diffusion occurring through the passivation. The magnitudes of the impedances were at 75 Ω/cm^2 for the Co-Free Mod and 100 Ω/cm^2 for the Co-Free passivation. The results from the Nyquist and Bode plots provide insight into the possible structure and properties of the passivations. For the CeCCs, the passivations were simple passive barriers. The CrCC and TCP passivations were more chemically activity, seen in the Bode plot, but also appeared to be strong passive barriers to corrosion, which is seen on the Nyquist plot. Co-Free and Co-Free Mod passivations were more chemically active, but did not provide a chemically noble barrier to corrosion.

Equivalent circuit (EC) models were used to analyze the EIS responses and determine the passivation structures and corrosion resistances. The EC models are depicted in Figure 5 and the componet values are tablulated in Table 3. The models all had an inductance term (L) of around 1.9 μH, thought to be due to the wiring of the cell configuration. The responses also all had R_e values that were consistantly around 7.2 Ω, which represents the resistance of the electrolye. The ECs (models A, B, and C) of the CeCCs, TCP, and CrCC were the simplest and were made up of a series of Randles circuits. Both CeCCs had only a single Randles circuit, TCP has two Randles circuits in series, CrCC has two or three Randles circuits in series. A Randles circuit represents an electrochemical reaction, which in the case of CeCCs is between the CeCC and the electrolyte. In the case of CrCC, the passivation is electrochemically active, having the ability to release hexavalent chromium to self-heal. This activity is seen with the two or three Randles circuits needed to model the response of the passivation. The added Randles circuits model the electrochemical reactions occuring with the bulk of the passivation.

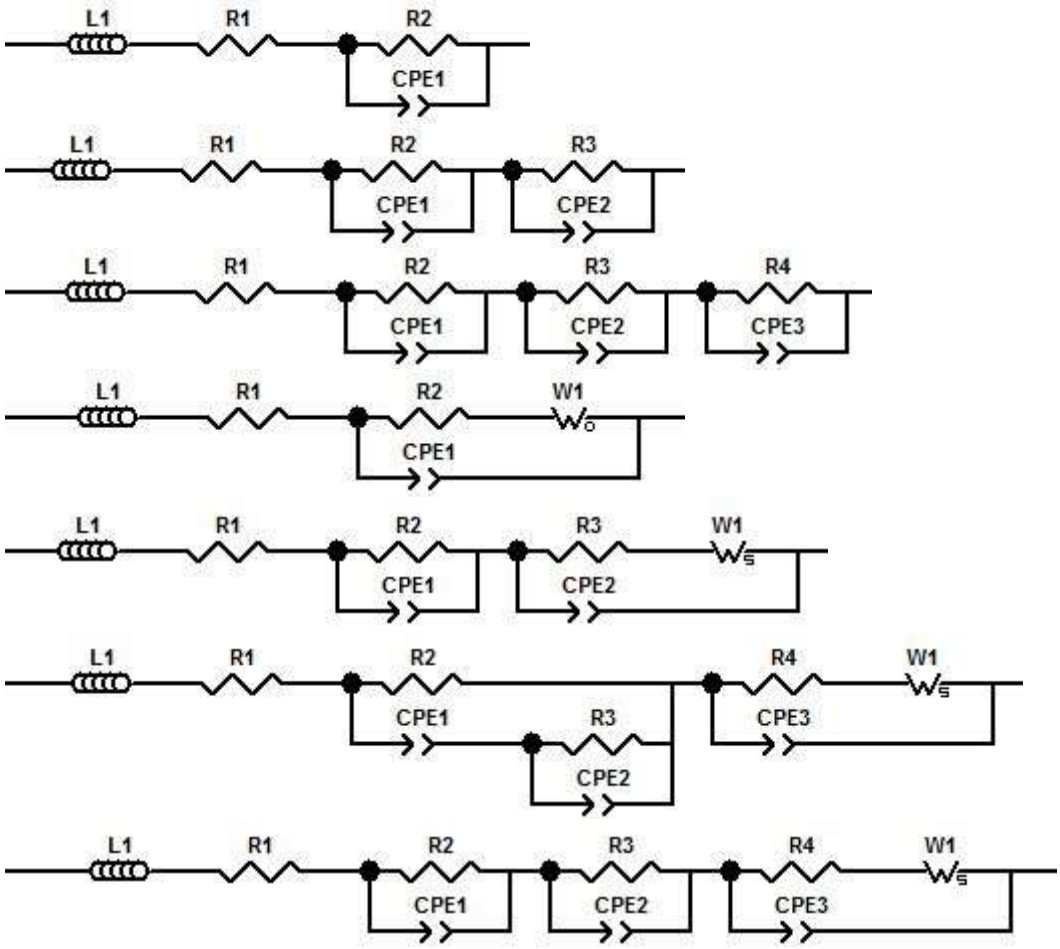

Figure 5: Equivalent Circuits; A) model for CeCCs, B) model for TCP coatings, B and C) models for CrCC, D-F) models for Co-Free coating, F and G) models for Co-Free Mod passivations.

The other peak likely represents the releasable hexavalent chromium, which was seen at high frequency, around 10^4 Hz. The Co-Free and Co-Free Mod coatings had similar ECs (Models D-G). The ECs all contained a Warburg diffusion componet that was needed to fit the circuits to the EIS data. Warburg diffusion is usually indicated by a linear section in the low frequency regime of the Nyquist plot.The linear section is at a 45˚ angle in the case of ideal behavior, but can vary in non-ideal cases.[31] Both of these passivations had these features on the Nyquist plot (Figure 4). All the ECs required a Warburg term in order to fit the experimental measurements; however, during testing the passivations had responses that required that different models to be used. Co-Free required three models to be used

and Co-Free Mod required two models. From the models, the passivations can be considered non-homogenous over the surface of the sample. This behavior will be discussed below with relation to salt spray testing.

Table 3: Equivalent Circuit Values

Coating	Model	L	R_e	R_p	CPE_{dl}		R_3	CPE_2		R_4	CPE_3		Warburg		
					C_{dl}	θ_{dl}		C_2	θ_2		C_3	θ_3	W_R	W_T	W_θ
CeCC-C1	A	$2.0x10^{-6}$	7.3	166	$4.4x10^{-3}$	0.79									
CeCC-N	A	$1.9x10^{-6}$	7.3	283	$2.2x10^{-3}$	0.77									
TCP	B	$1.7x10^{-6}$	7.1	363	$1.8x10^{-3}$	0.68	14	$1.6x10^{-3}$	1.05						
CrCC	B	$1.6x10^{-6}$	6.7	66	$5.3x10^{-3}$	0.51	337	$4.3x10^{-3}$	0.87						
	C	$2.0x10^{-6}$	6.8	37	$1.6x10^{-3}$	0.69	543	$2.2x10^{-3}$	0.81	3	$2.9x10^{-4}$	0.70			
	D	$2.0x10^{-6}$	7.4	24	$2.4x10^{-3}$	0.85							51	33	0.23
Co-Free	E	$2.1x10^{-6}$	7.9	7	$1.3x10^{-3}$	0.74	81	$9.2x10^{-3}$	0.78				93	38	0.46
	F	$2.1x10^{-6}$	7.5	24	14	4.17	76	$4.4x10^{-3}$	0.48	16	$1.2x10^{-2}$	1.00	149	52	0.52
Co-Free Mod	F	$1.8x10^{-6}$	6.3	156	$7.2x10^{-2}$	0.55	12	$1.2x10^{-1}$	0.92	9	$8.4x10^{-4}$	0.89	9	0.3	0.24
	G	$2.0x10^{-6}$	7.2	6	$1.3x10^{-3}$	0.89	274	$6.6x10^{-2}$	0.52	9	$8.3x10^{-4}$	1.04	25	3	0.46

After corrosion

Figure 6 shows the passivated panels after 1000 hours of salt spray testing. The TCP panel changed color, but did not show any other visible signs of corrosion. Co-Free Mod developed a small amount of corrosion product on the surface. CrCC and Co-Free passivations had moderate amounts of corrosion product form. The CeCCs had the most corrosion product development. The CrCC, Co-Free and Co-Free Mod had non-uniform development of corrosion product, with Co-Free having a large area on the panel having more corrosion than the other.

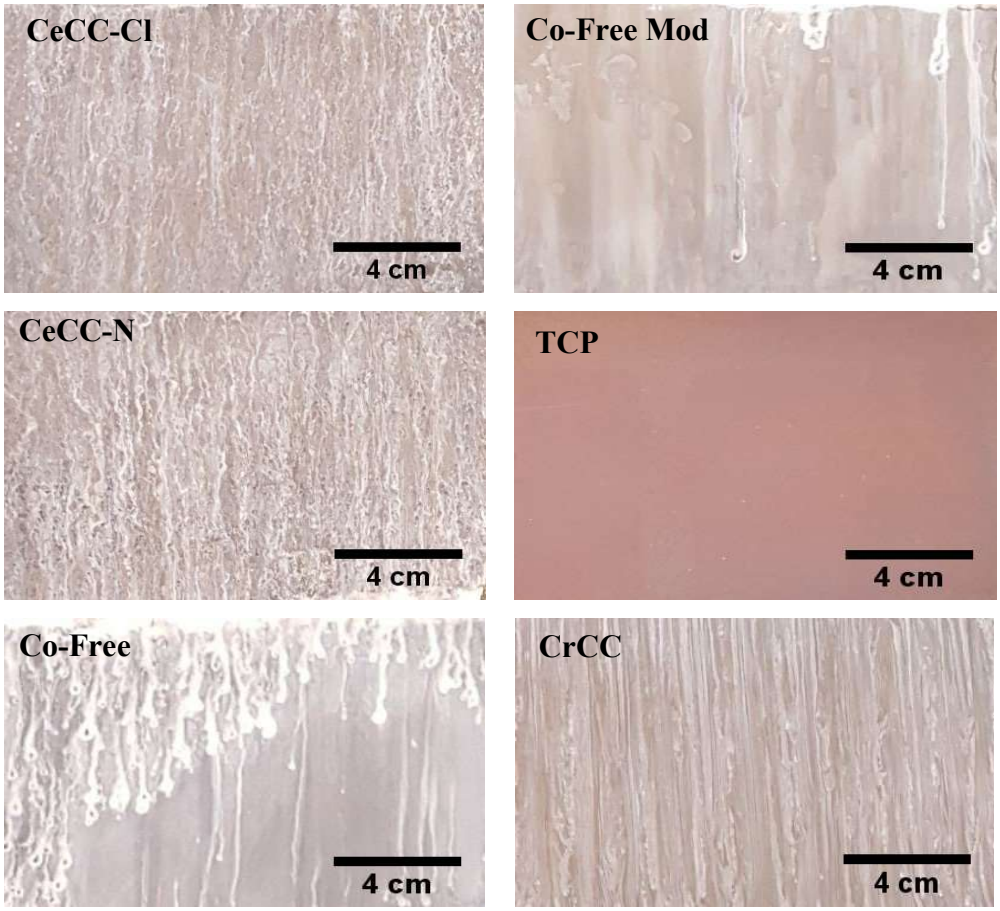

Figure 6: Passivation coatings on γ-ZnNi panels after 1000 hrs. exposure to salt spray testing.

The CrCC and Co-Free Mod passivations developed more corrosion product in what looked like bands across the panel surface with some areas corroded and others not corroded. This is thought to occur because of the passivation having multiple EIS responses in different locations across the surface. The uniform corrosion development on the CeCCs and the TCP passivations was predicted by the EC models. The results showed a strong correlation between the EIS tests before corrosion occurred and the salt spray testing, where the panels with a uniform complex response had good performance in salt spray. The panels that stood out from the testing were the TCP and Co-Free Mod panels, which showed limited corrosion.

After corrosion, EIS data (Figure 7) showed all of the passivations broke down to simple barriers after salt spray testing. This was concluded from the shape of the curves on the Bode plots, where all the passivations had a single time dependence, which resulted in a single peak for each passivation. Compared to the as-deposited panels, the impedance magnitude was higher for all passivations after corrosion, except for CrCC, which decreased from 500 Ω/cm^2 to 250 Ω/cm^2. The Co-Free and Co-Free Mod passivations no longer show a Warburg diffusion dependence. TCP and Co-Free Mod changed the least during exposure, both had a slight increase in their impedance values from about 75 Ω/cm^2 to about 160 Ω/cm^2. This slight change is also seen visually, with the samples having no or slight corrosion product development on the samples (Figure 6).

The Co-Free Mod passivation had a contact resistance of 1 $m\Omega/cm^2$ after 1000 hours in salt spray. This was the only passivation that was able to maintain a contact resistance below the military requirement of 1.6 $m\Omega/cm^2$ after corrosion. The next lowest

contact resistance was demonstrated by TCP at 3 mΩ/cm^2, which was just above the requirement.

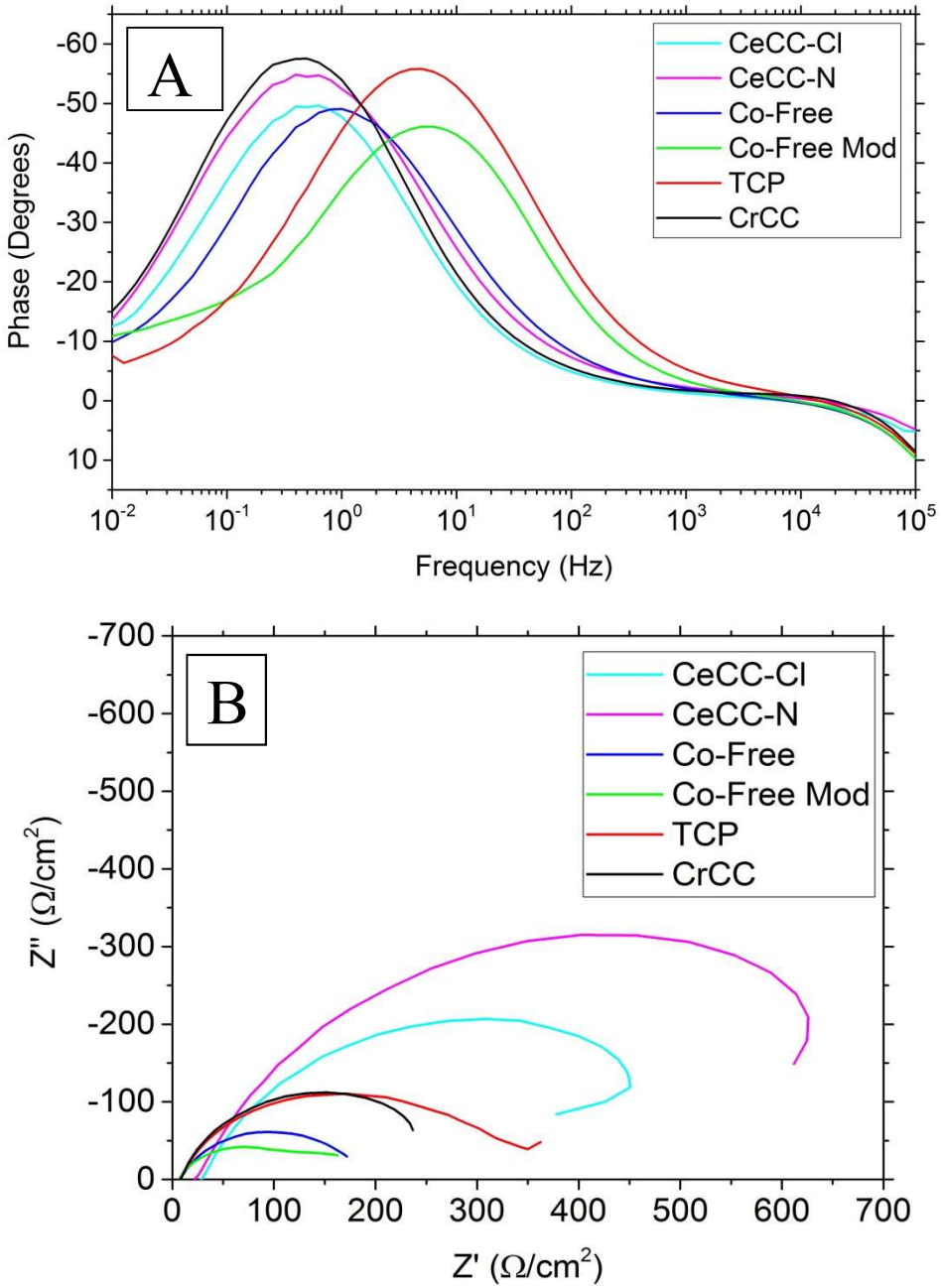

Figure 7: A) Bode plot for corroded passivations after 1000 hrs. of salt spray testing. B) Nyquist plot of passivations after 1000 hrs. of salt spray testing.

The rest of the passivations had contact resistance values ranging from ~4700 mΩ/cm^2 to 10^8 mΩ/cm^2. From the previous observations, the Co-Free Mod and TCP passivations showed the least amount of corrosion product on the surfaces, which was consistent with them having the lowest contact resistances. The increase in contact resistance on the other passivations was due to accumulation of electrically insulate corrosion product on the panel surfaces.

Table 4: Contact Resistances After 1000 hrs. of SST

	After SST
	mΩ/cm^2
CeCC-Cl	$1 \times 10^8 \pm 5 \times 10^7$
CeCC-N	$9 \times 10^7 \pm 3 \times 10^7$
Co-Free	$3 \times 10^4 \pm 3 \times 10^4$
Co-Free Mod	1 ± 0.6
TCP	3 ± 1
CrCC	$5 \times 10^3 \pm 2 \times 10^3$

Conclusions

The corrosion behavior and contact resistances were characterized for six different passivations on electroplated ZnNi. These passivations were compared before and after SST using electrochemical analysis and electrical contact resistance measurements. The electrochemical analysis revealed that the more electrochemically active chromium-based passivations performed better in SST. Results from EIS indicated that the coatings broke down into simple corrosion barriers after SST. The electrical contact resistance of the coating systems after SST also followed the same pattern with the lowest measured resistances coming from the more active chromium-based passivations. Both the Co-Free Mod and TCP coating systems were able to inhibit corrosion and maintain low contact resistances through 1000 hours of SST.

Acknowledgements

This work was funded by the Strategic Environmental Research and Development Program (SERDP) under contract. The authors would like to acknowledge the support of Dr. Robin Nissan at SERDP along with Stephen Gaydos of Boeing for providing his expertise. We also would like to thank Dr. Tarek Nahlawi of Dipsol of America for providing the all of the electroplated ZnNi on steel panels and the chromium-based passivated panels. Also, we give much appreciation to Ron Haas for building the contact resistance measuring device and for use of equipment.

References

[1] Tom Naguy, George Slenski, Robert Keenan, G. Chiles, D.o. Defense (Ed.) 1998.

[2] D.o. Defense, Detail Specification Chemical Conversion Materials For Coating Aluminum And Aluminum Alloys, in: D.o. Defense (Ed.) 2002.

[3] Dayanne Dutra de Menezes, L.S., Sylvio Jose Riberio de Oliveria, L.C.V.d. Castro.

[4] M.W. Kendig, R.G. Buchheit, Corroison Science 59(5) (2003) 379-400.

[5] OSHA, Chromium (VI), in: O.S.a.H. Administration (Ed.) 1910.1026.

[6] A. Conde, M.A. Arenas, J.J. Damborenea, Corrosion Science 53 (2011) 1489-1497.

[7] K. R. Baldwin, M. J. Robinson, C.J.E. Smith, Corrosion Science 35 (1993) 1297-1272.

[8] Moonjae Kwon, Soo Hyoun Cho, Yuan Tae Kim, Jong-Tae Park, J.M. Park, Surface & Coating Technology 288 (2016) 163-170.

[9] A.Y. Polyakov, N.B. Smirnov, A.V. Govorkov, E.A. Kozhukhova, S.J. Pearton, D.P. Norton, A. Osinsky, A. Dabiran, Journal of Electronic Materials 35(4) (2006) 663-669.

[10] E. Akiyama, A. J. Markworth, J. K. McCoy, G. S. Frankel, L. Xia, R.L. McCreery, Journal of the Electrochemical Society 150(2) (2003) B83-B91.

[11] Simon Joshi, Elizabeth, A. Kulp, William G. Fahrenholtz, M.J. O'Keefe, Corrosion Science (60) (2012) 290-295.

[12] T.J. Haley, Journal of Pharmaceutical Sciences 54(5) (1965) 663-670.

[13] Becky L. Treu, Simon Joshi, William R. Pinc, Matthew J. O'Keefe, W.G. Fahrenholtz, Journal of the Electrochemical Society 157(8) (2010) C282-C287.

[14] Carlos E. Castano, Matthew J. O'Keefe, W.G. Fahrenholtz, Current Opinion in Solid State and Material Science 19 (2015) 69-76.

[15] Daimon K. Heller, William G. Fahrenholtz, M.J. O'Keefe, Journal of the Electrochemical Society 156 (2009) C400-C406.

[16] William G. Fahrenholtz, Matthew J.O'Keefe, Haifeng Zhou, J.T. Grant, Surface & Coating Technology 155 (2002) 208-213.

[17] Yuanyuan Liu, Jiamu Huang, James B. Claypool, Carlos E. Castano, M.J. O'Keefe, Surface Engineering 355 (2015) 805-813.

[18] A. Aballe, M. Bethencourt, F. J. Botana, M.J. Cano, M. Marcos, Materials and Corrosion 53 (2002) 176-184.

[19] M. G. Hosseini, H. A. Y. Ghiasvand, H. Ashassi-Sorkhabi, Surface Engineering 29(1) (2013).

[20] K. Aramaki, Corroison Science 43 (2001) 2201-2215.

[21] N. Geographic, Ocean Acidification. <http://ocean.nationalgeographic.com/ocean/explore/pristine-seas/critical-issues-ocean-acidification/>, 2016 (accessed 9/16.2016).

[22] N.T. Wen, F.J. Chen, M.D. Ger, Y.N. Pan, C.S. Lin, Electrochemical and Solid State Letters 11(8) (2008) C47-C50.

[23] X. Zhang, C. van den Bos, W.G. Sloof, A. Hovestad, H. Terryn, J.H.W.d. Wit, Surface Engineering 20(4) (2004) 244-250.

[24] Yu-Tsern Chang, Niann-Tsyr Wen, We-Kun Chen, Ming-Der Ger, Guan-Tin Pan, T.C.-K. Yang, Corroison Science 50 (2008) 3494-3499.

[25] T. Bellezze, G. Roventi, R. Fratesi, Surface & Coating Technology 155 (2002) 221-230.

[26] Niann-Tsyr Wen, Chao-Sung Lin, Ching-Yuan Bai, M.-D. Ger, Surface and Coatings Technology (203) (2008) 317-323.

[27] Robert Berger, B. Ulf, T. Mikeal Grehk, S.-E. Hornstrom, Surface & Coating Technology (202) (2007) 391-397.

[28] KuenWoo Cho, V. Shankar Rao, H. Kwon, Electrochimica Acta (52) (2007) 4449-4456.

[29] X. Zhang, C. van den Bos, W.G. Sloof, A. Hovestad, H. Terryn, J.H.W.d. Wit, Surface & Coating Technology (199) (2005) 92-104.

[30] John A. Thornton, D.W. Hoffman, Thin Solid Films 171(1) (1989) 5-31.

[31] Jun Huang, Zhe Li, Bor Yann Liaw, J. Zhang, Journal of Power Sources 309 (2016) 82-98.

II. CHARACTERIZATION OF ELECTROPLATED γ-ZnNi WITH PASSIVATION LAYERS

S. M. Volz, J. B. Claypool, M. J. O'Keefe, W. G. Fahrenholtz

Materials Research Center, Department of Materials Science and Engineering, Missouri University of Science and Technology, Rolla, MO 65401, USA

ABSTRACT

The microstructure and chemical composition of passivation coatings deposited on low hydrogen embrittlement electroplated γ-ZnNi were investigated. Trivalent chromium-based passivations and cerium-based passivations were compared to hexavalent chromium-based passivation before and after ASTM B117 salt spray exposure. The results indicated that changes in appearance and performance occurred as the exposure time in salt spray increased and that the passivations influenced the microstructure of the corrosion product. Cerium-based passivations formed a rounded corrosion product structure, while the morphology of the corrosion product on trivalent chromium-based passivations was plate-like. The chemical compositions and amounts of the corrosion product varied between passivations. Trivalent chromium-based passivations provided the best resistance to corrosion based on the lower levels of zinc hydroxycarbonate produced during salt spray exposure.

Introduction

Coatings based on gamma phase zinc nickel (γ-ZnNi) are environmentally-friendly replacements for cadmium coatings.[1-5] For example, γ-ZnNi coatings are replacing cadmium coatings on electrical connectors for U.S. Department of Defense (DoD) systems because of desirable properties such as corrosion resistance, hardness, wear resistance, electrical resistance, and coefficient of thermal expansion (CTE) compatibility that are similar to cadmium.[6, 7] Coatings based on γ-ZnNi are sacrificial to steel in a corrosive environment and have relatively low corrosion rates.[1, 3, 4] Unlike cadmium, which is toxic, γ-ZnNi is environmentally benign.[8] Similar to cadmium coatings, γ-ZnNi coatings can also undergo post-deposition heat treatments to mitigate potential issues with hydrogen embrittlement.[9]

To maintain the desired contact resistance for electrical connectors, γ-ZnNi coatings require a passivation coating to minimize the formation of electrically insulating corrosion products.[10] Currently, chromate conversion coatings (CrCCs) are the only approved passivation for use with γ-ZnNi in DoD systems.[6] No non-CrCC passivations have consistently demonstrated the ability to maintain contact resistance values that meet DoD specifications before and after salt spray exposure.[6] Corrosion protection of CrCCs involves the release hexavalent chromium (Cr^{6+} or chromate ions); however, chromates are carcinogenic and the subject of strict workplace limitations (OSHA 1910.1026).[11] Hence, environmentally-friendly passivation are needed for γ-ZnNi coatings.

Cerium-based conversion coatings (CeCCs) are an environmentally-friendly alternative to CrCCs that are being studied for corrosion protection of several different alloys. [12-17] Due to their low solubility over a wide range of pH, CeCCs have been used

for corrosion protection for several different applications.[18] Cerium compounds are environmentally benign, having only a low to moderate toxicity when tested in animals.[19] The low solubility and the environmentally friendly nature of cerium compounds makes them promising candidates to replace CrCCs.

Cerium-based conversion coatings can be deposited by spontaneous or electrolytic means from chloride or nitrate cerium salts in either aqueous or organic solvents.[12-15, 20] Several different corrosion protection mechanisms have been proposed for CeCCs including acting as insoluble barrier, redox involving Ce^{4+} and Ce^{3+} complexes,[12-15, 20] inhibiting transport of O_2, and inhibiting the cathodic half-reaction.[21, 22] One previous study also noted the corrosion protection of CeCCs on δ-ZnNi was comparable to that of CrCCs on the same substrate.[22]

Trivalent chromium-based passivations (TCPs) have also been studied as potential replacements for CrCCs.[23-26] Although TCP coatings contain chromium, trivalent Cr^{3+} ions are considered to be much less toxic than hexavalent Cr^{6+} ions.[27] Studies have found that TCP-based passivations on zinc are corrosion resistant, but due to a lack of self-healing ability, the corrosion performance of TCP-based coatings is inferior to CrCCs.[28] The structure and properties of TCP coatings can be altered with different anions in the deposition solution.[29] For example, sulfate anions produced coatings with large grains, whereas nitrate and chloride anions produced coatings with fine grain sizes.[29] In general, TCP coatings are stable and have low solubility in corrosive environments, thus providing a barrier to corrosion.[24]

The purpose of this study was to characterize environmentally friendly passivations that are potential replacements for CrCCs currently used on γ-ZnNi coatings on electrical connectors.

Procedure

Six different passivations for γ-ZnNi coatings were evaluated. The γ-ZnNi coatings contained approximately 14 wt% nickel, were about 10 μm thick, and were deposited on steel substrates. The passivations that were compared were: 1) a commercially available TCP coating (IZ-264, Dipsol of America, Livonia, MI); 2) a cobalt-free TCP (Co-Free) that is under development by Dipsol; 3) a modified cobalt-free TCP (Co-Free Mod) also under development by Dipsol; 4) a commercially available CrCC coating (IZ-258, Dipsol of America, Livonia, MI); 5) a CeCC deposited from a chloride-based solution (CeCC-Cl); and 6) a CeCC deposited from a nitrate-based solution (CeCC-N). Passivations 1-4 were provided already deposited on electroplated γ-ZnNi steel substrates. Additional steel substrates electroplated with γ-ZnNi were also provided by Dipsol for the deposition of CeCCs.

Deposition of cerium-based passivations

The γ-ZnNi substrates were first wiped clean with ethanol. The substrates were then immersed in a 5 wt% aqueous solution of an alkaline cleaner (Turco 4215 NC-LT, Henkel) at 55˚C for 5 minutes to degrease the surface. After degreasing, panels were rinsed with deionized (DI) water. A 0.037 mol/L HCl solution in DI water was used for surface activation. Panels were immersed for 30 seconds at room temperature and then rinsed with DI water. Next, cerium-based passivations were deposited from either one of two deposition baths, one based on cerium chloride or a second based on cerium nitrate. The cerium chloride bath consisted of 4.2 wt% cerium chloride hexahydrate (Alfa Aesar, 99.9%, Ward Hill, MA), 4.2 wt% (Fisher Scientific, 34-37% technical grade, Fair Lawn, MA) hydrogen peroxide solution and 0.3 wt% (Rousselot DSF, Dubuque, IA) gelatin in DI

water. The cerium nitrate bath consisted of 4.8 wt% cerium nitrate heptahydrate (Acros Organics, 99.5%, Geel, Belgium), 4.1 wt% (Fisher Scientific, 34-37% technical grade, Fair Lawn, MA) hydrogen peroxide and 0.3 wt% (Rousselot DSF, Dubuque, IA) gelatin in an aqueous solution. The substrates were immersed in either bath at a pH of 2 for 2 minutes at room temperature. Post-treatment of the cerium passivations was done in a 2.5 wt% sodium phosphate monobasic dihydrate (Fisher Scientific, 99.8%, Fair Lawn, NJ) solution at 85˚C of 5 minutes and then rinsed with DI water. The panels were allowed to air dry for at least 24 hours before testing.

Characterization and corrosion testing

Corrosion resistance was evaluated in salt spray testing (SST; Q-fog, Q-Panel Lab products, Westlake, OH) performed according to ASTM B117. A 5 wt% sodium chloride aqueous solution was used in the chamber, as specified in the standard. Testing was performed on each of the coatings for up to 1000 hours. Coatings were visually evaluated at 100-hour intervals.Scanning electron microscopy (SEM; S-4700, Hitachi, Japan) was performed to look at the microstructure of the passivations before and after SST. Images were taken using an accelerating voltage of 15 keV. Energy-dispersive X-ray spectroscopy (EDS) (Apollo X, EDAX, Mahwah, NJ) was performed in the SEM to analyze chemical composition. A dual beam system (Helios Nanolab 600, FEI, Hillsboro, OR) with SEM and focused ion beam (FIB) milling capabilities was used to produce and examine cross sections of the coatings. Images were taken using an accelerating voltage of 5KeV. A digital optical microscope (KH-8700, Hirox, Hackensack, NJ) was used to determine the surface roughness of the electroplated ZnNi using automated image analysis. Glancing angle X-ray diffraction (X-pert Diffactometer, Phillips, Westborough, MA) was performed to determine the phases and composition of the coating system before and after SST.

Electrochemical impedance spectroscopy (EIS) was performed to study the electrochemical response of the electroplated ZnNi before passivation. A flat cell (model K0235, Princeton Applied Research, Oak Ridge, TN) and saturated calomel electrode were used. The electrolyte used was an aqueous solution containing 0.6 M ammonium sulfate and 0.6 M sodium chloride. Experiments were conducted using a potentiostat (EG&G Princeton Applied Research, Model 273A, Oak Ridge, TN) and a frequency response analyzer (Solartron Instruments, SI 1255, Oak Ridge, TN). The software used was for data collection and analysis using software packages (Zplot and Zview, Scribner Associates, Inc., Southern Pines, NC). Prior to analysis, the coatings were allowed to reach their open circuit potential over a time period of 2000 seconds before starting EIS, which was run over a frequency range of 10^{-2} to 10^{5} Hz with AC amplitude of 10 mV.

Results and discussion

Starting γ-ZnNi surface

The surface of the γ-ZnNi was not smooth as seen with the line profile in Figure 1. The line profile indicated that the deviation from the average height in the Z direction is 1.4 ± 0.4 μm. The surface morphology of the as-deposited γ-ZnNi on steel is depicted in Figure 2. The γ-ZnNi had a hemispherical-like appearance with submicron grains making up the hemispheres. Figure 3 shows a focused ion beam cross section of γ-ZnNi, the image revealed a vertically aligned grain texture, which has been reported by other studies.[30] The γ-ZnNi microstructure is dependent on the electrodeposition procedure used, and the hemispherical globular-like structure was also reported by others.[31] The images also showed that the coatings had pits at some of the hemisphere boundaries. These pits were likely caused by gas evolution during the deposition process.[32] Gas bubbles can adhere to the substrate, possibly blocking areas from contact with the deposition solution, causing

the γ-ZnNi to deposit around the bubble, which would produce a pit. The rough surface along with the pits could impact the many of the desired properties of the γ-ZnNi coatings, such as the electrochemical response. The γ-ZnNi coatings exhibit Warburg diffusion behavior in EIS as seen in Figure 4, which is consistent with the pits observed in the SEM images.[30] Warburg diffusion is seen as a linear section at a 45˚ phase angle at low frequencies on the Nyquist plot.

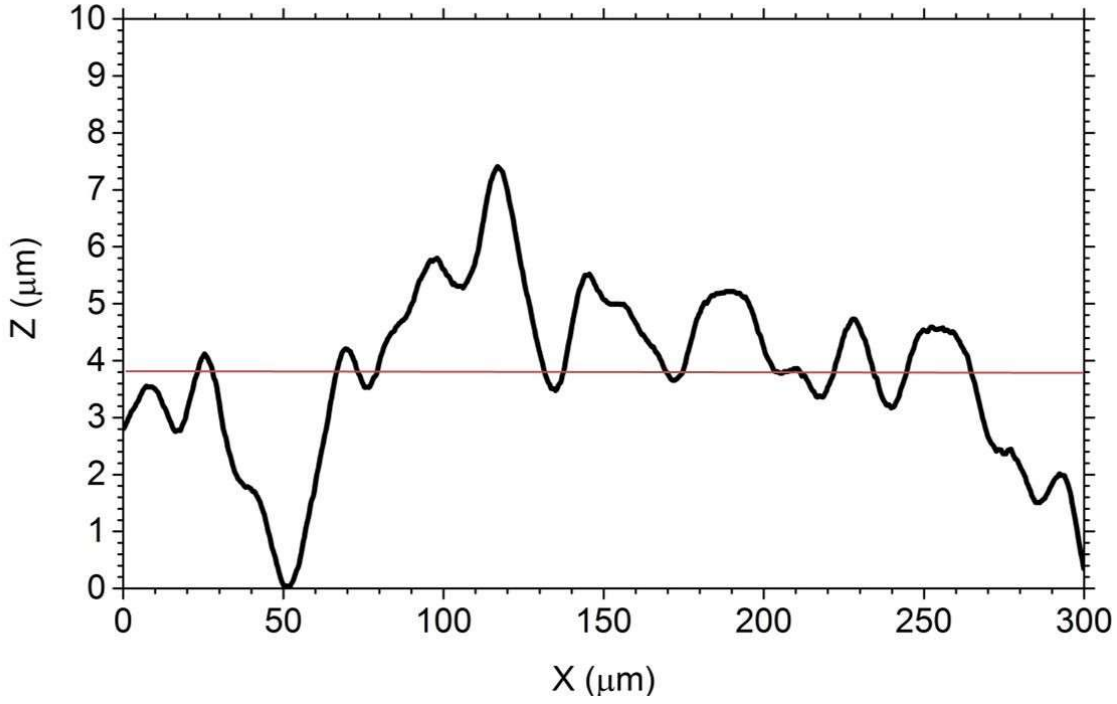

Figure 1: Surface roughness of as-deposited electroplated γ-ZnNi on steel. The red line represents the average height.

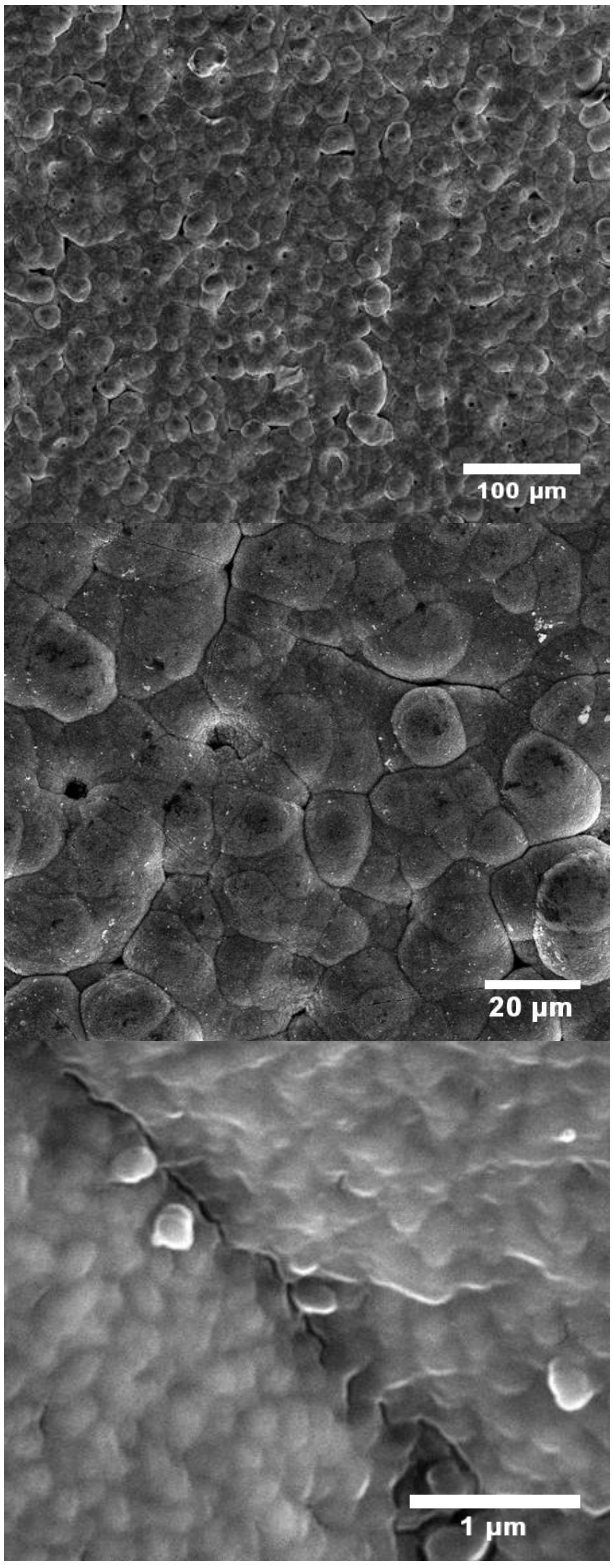

Figure 2: Surface morphology of as-deposited electroplated γ-ZnNi on steel at different magnifications.

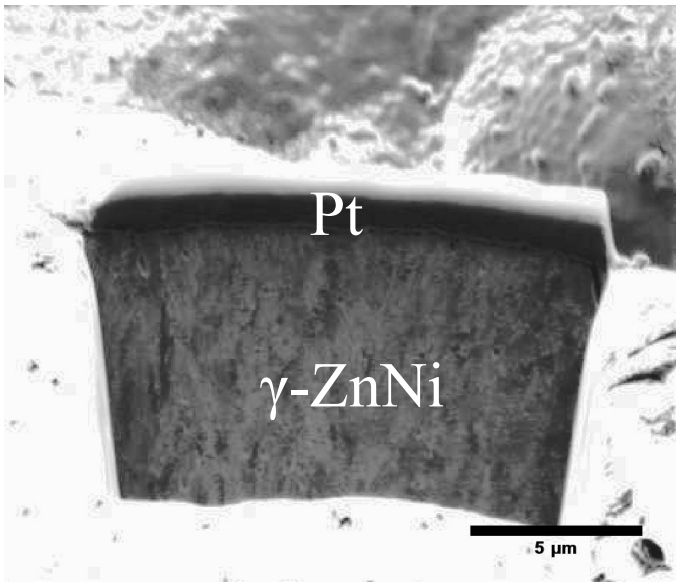

Figure 3: High contrast ion beam cross section image of γ-ZnNi.

This behavior correlates to the penetration of the electrolyte into the coating. The electrochemical species have to diffuse through the pit in order to reach equilibrium in the bulk electrolyte solution.[33] Whereas in a uniform pristine coating the species produced at the surface can immediately go into the bulk solution and would eliminate the Warburg diffusion behavior. This interpretation of Warburg diffusion is an example of how surface morphology can control the electrochemical response of the coating.

The phase and crystal structure for the electrodeposited γ-ZnNi coating were confirmed with XRD, Figure 5. The pattern established that the phase was stoichiometric Ni_2Zn_{11}, which is consistent with the composition of γ-ZnNi. The pattern showed that the diffraction peak corresponding to the (303) plane was more intense than expected for a randomly oriented polycrystalline material. The higher intensity of this peak was consistent with texturing of the coating along that crystallographic direction, which can be explained by the anisotropic grains seen in the ion beam cross section, Figure 2.[34]

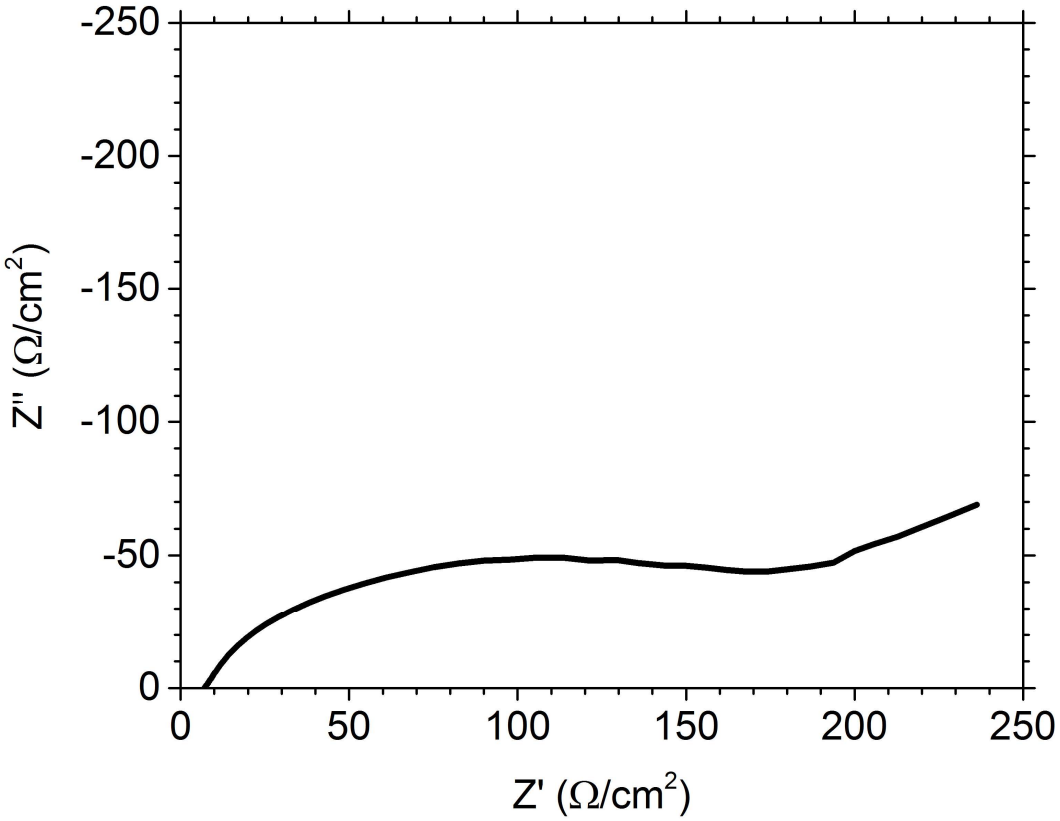

Figure 4: Electrochemical impedance spectroscopy Nyquist plot for as-deposited electroplated γ-ZnNi on steel.

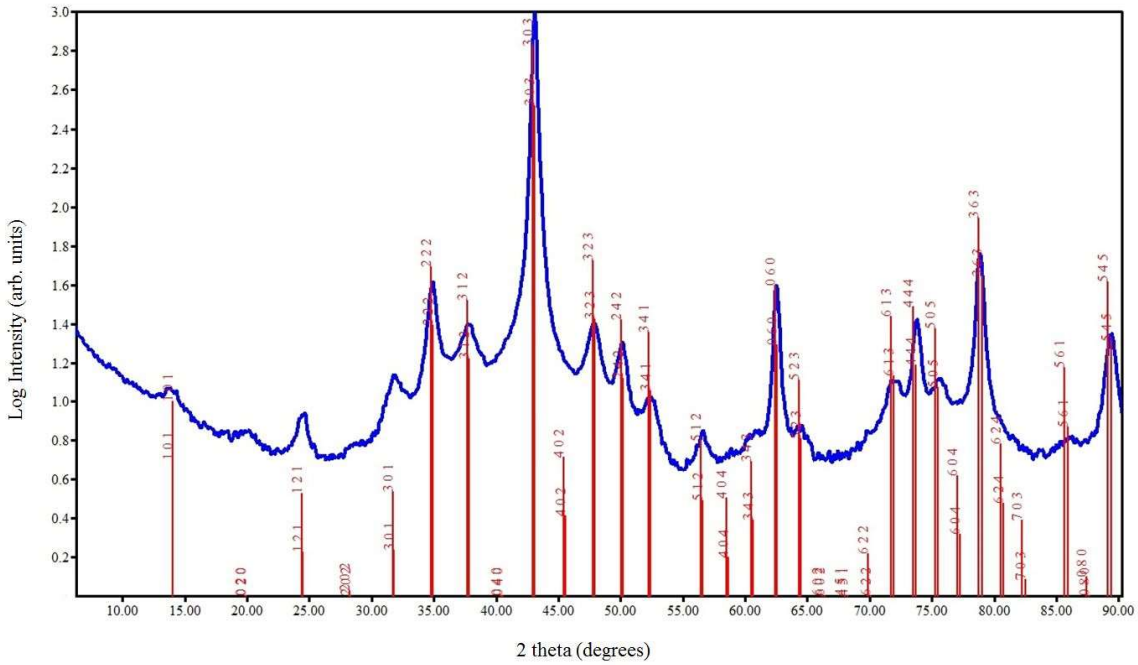

Figure 5: XRD pattern for electroplated γ-ZnNi coating.

As-deposited passivations

All passivations uniformly covered the panels with only very slight coloring differences seen in Figure 6. Co-Free and Co-Free Mod passivations were grayish yellow while the CeCC-Cl and CrCC passivations were golden yellow with areas of varying color. CeCC-N and TCP had a golden color, but with areas of dark blue. The different areas of color could be attributed to coating thickness variance and compositional differences, which was discussed in detail in a previous study.[35]

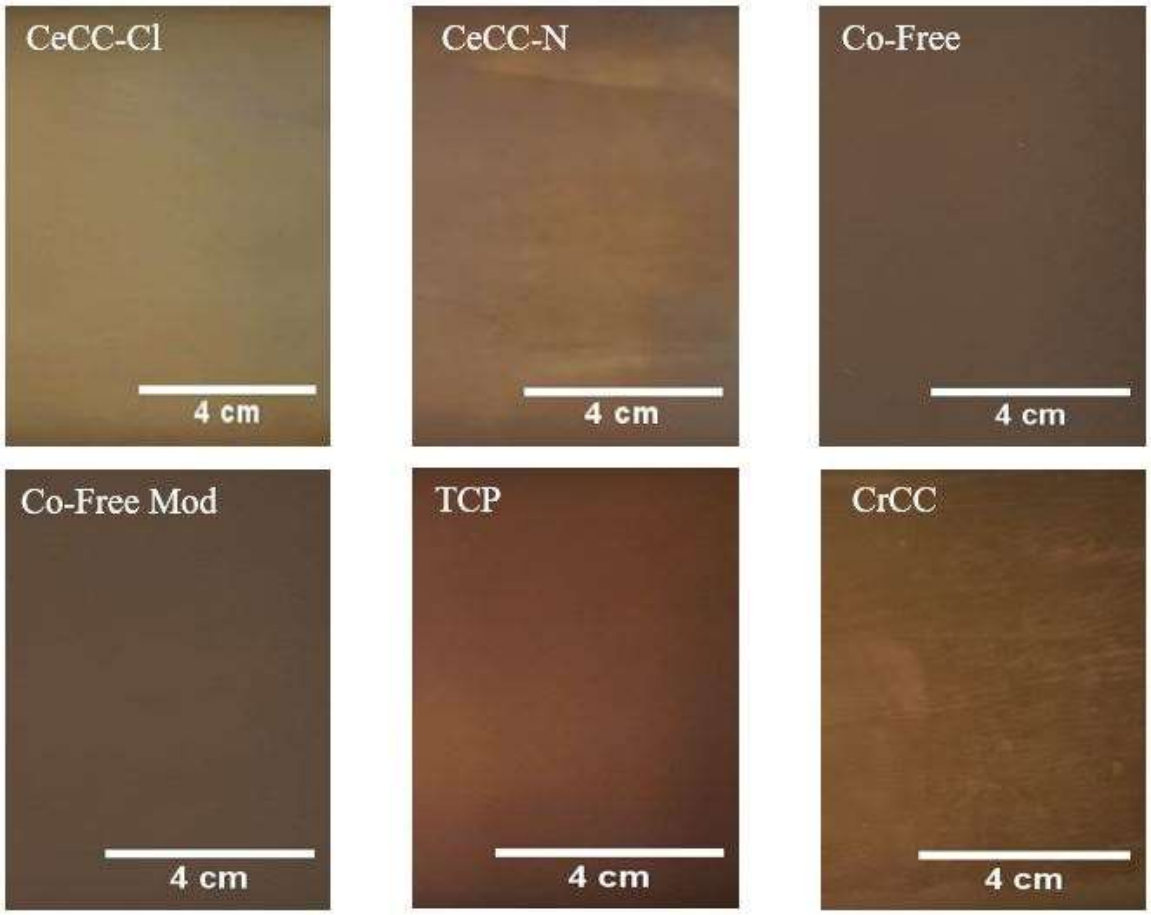

Figure 6: Optical micrographs showing the surface morphology of γ-ZnNi panels with different as-deposited passivations

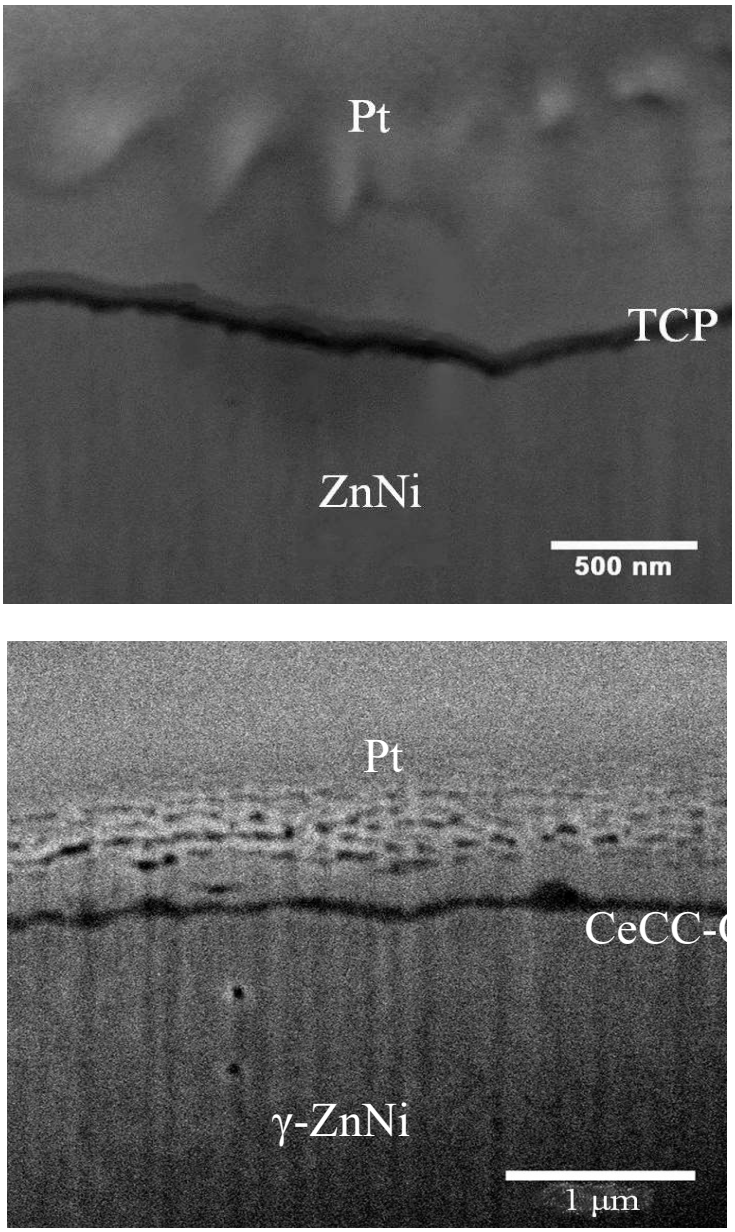

Figure 7: SEM cross section of A) TCP coated γ-ZnNi and B) CeCC-Cl coated γ-ZnNi. Note that the images are different magnifications.

Figure 7 shows cross section TCP (A) and CeCC-Cl (B) passivations on γ-ZnNi coatings. Both of the passivations had an average thickness of about 100 nm, which is assumed to be similar for the other passivations based on measured electrical resistances reported in a previous study.[35] The passivations are approximately two orders of magnitude thinner than the γ-ZnNi coatings and form a uniform conformal layer over γ-ZnNi. Grazing

incidence XRD was used in an attempt to characterize the crystalline phases in the passivations, but only the underlying γ-ZnNi coatings were detected due to the roughness of the γ-ZnNi, the nanocrystalline nature of the passivations, and thin passivation layers.

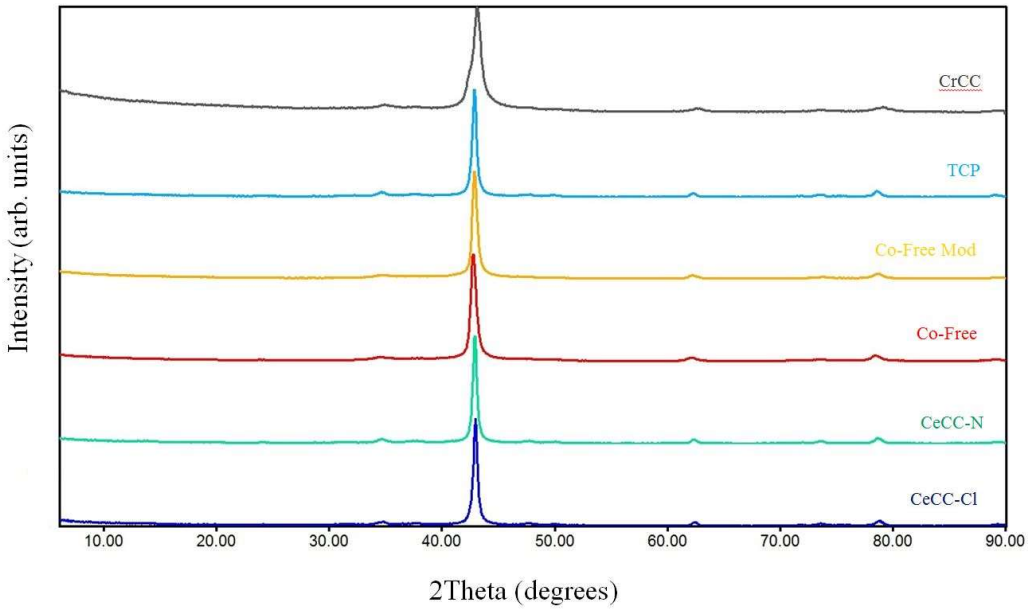

Figure 8: XRD of as-Deposited passivations.

After salt spray testing

Images of the passivated panels after salt spray testing (SST) are shown in Figure 9. The coatings did not corrode uniformly during SST. For example, Co-Free had areas significant build-up of corrosion product, whereas a large area of the panel was covered with only a thin whitish coating of corrosion product. The same non-uniformity was seen to a lesser degree on both Co-Free Mod and CrCC. Co-Free Mod has a few small areas with more corrosion product compared to the rest of the panel. As for CrCC, the corrosion developed what looked like stripes of high concentrations of corrosion product alternating with regions of lower amounts of corrosion product. Compared to the development of corrosion products on the CeCCs and TCP, these passivations had very non-uniform

corrosion product layers. The CeCCs developed what looks to be a thicker corrosion product layer that covered more of the surface of the panel compared to the other passivations. TCP was the only passivation that seemed to produce very little, if any, corrosion product, but did become noticeably lighter in color after SST. All the coatings had visually macroscopic differences, when they were compared after SST, demonstrating that the passivations type and even processing differences in the same type of passivations affected the amount and appearance of the corrosion products.

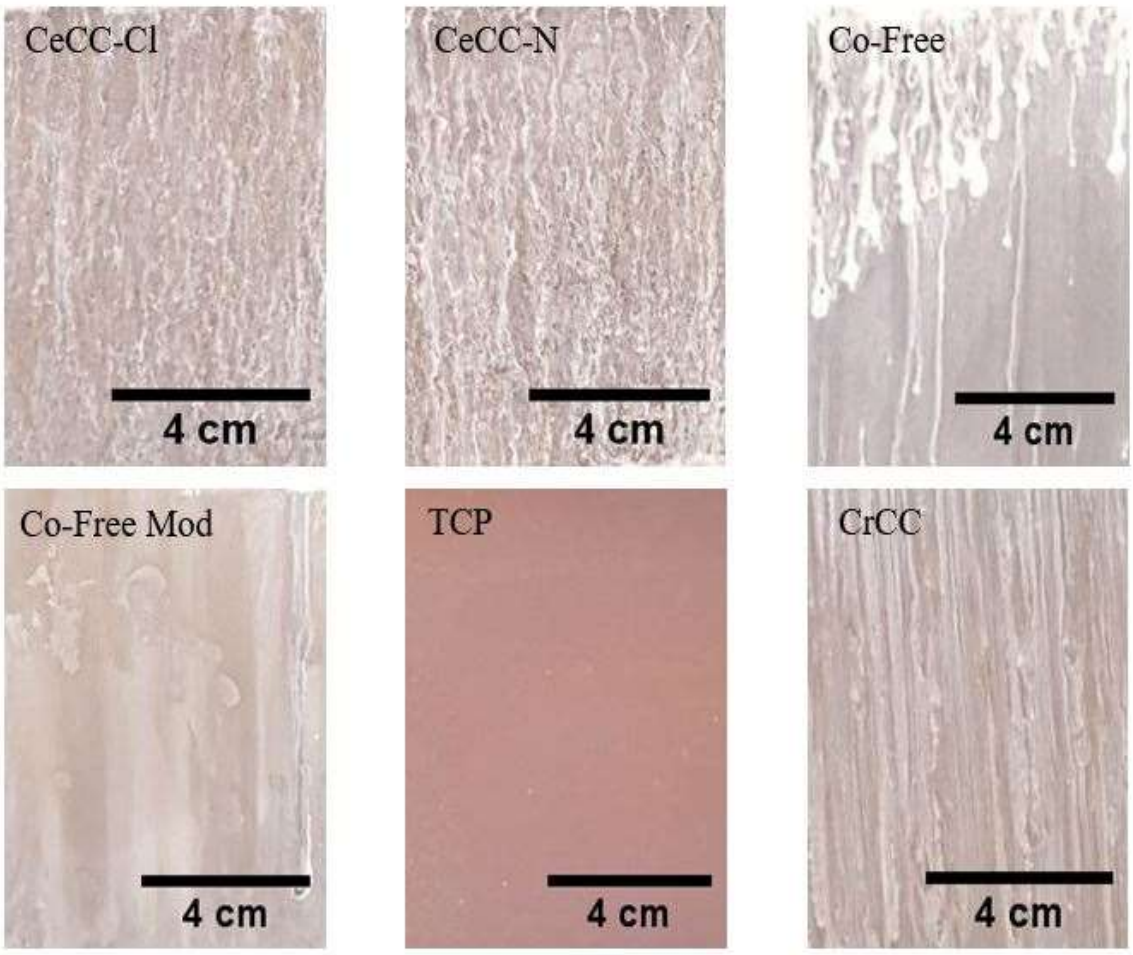

Figure 9: Optical micrographs showing the surface morphology of γ-ZnNi panels with different passivations after 1000 hrs. of SST.

The difference appearances of the passivations after SST can be seen also at the microscopic level. Figures 10 and 11, show examples of microstructures of passivations after SST with corrosion products on the surfaces. The microstructures varied widely among the different types of passivations. The CeCCs developed a rounded structure with crystals of corrosion product. In contrast, Co-Free had plate-like crystals of the corrosion product while Co-Free Mod developed pits and had what looked to be the start of the plate-

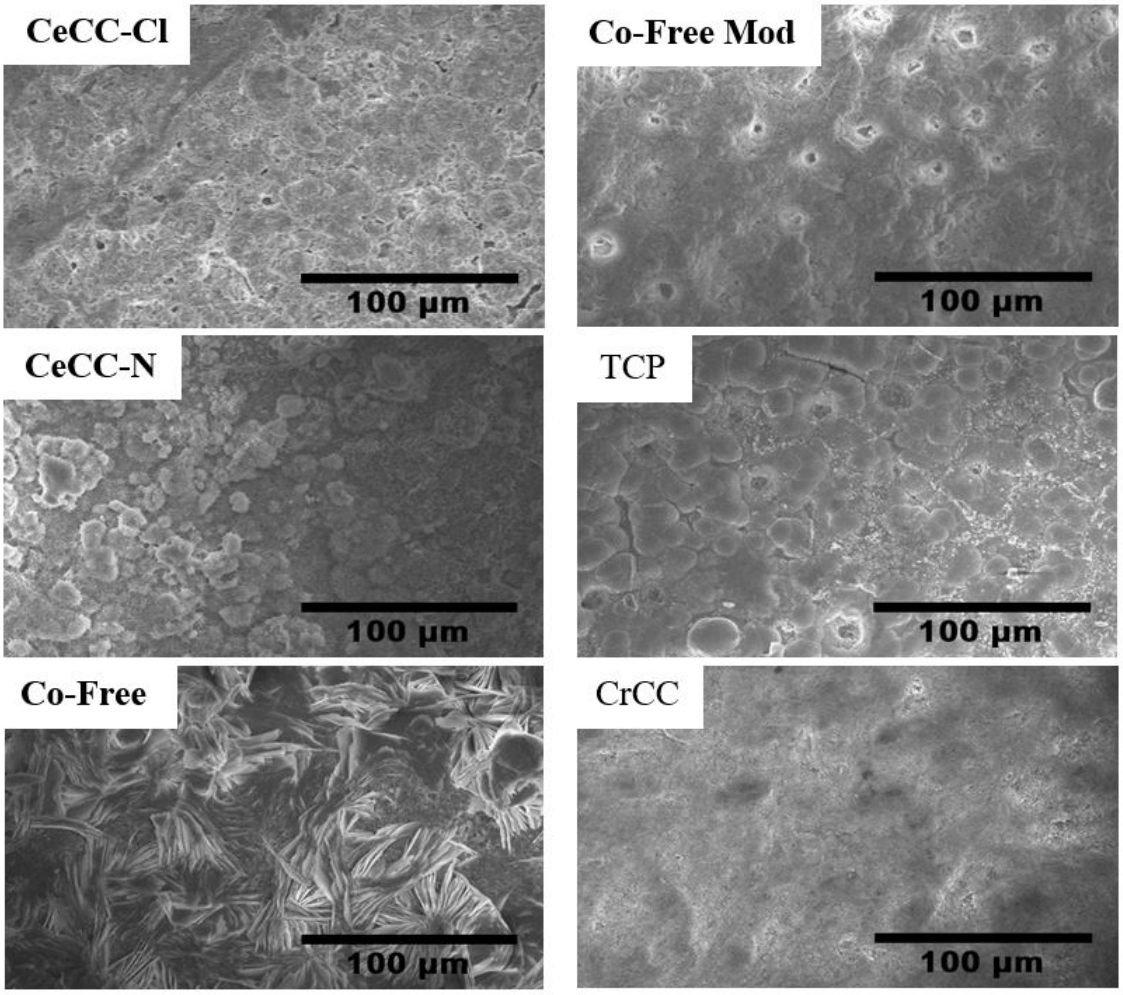

Figure 10: Surface morphology at 500x of γ-ZnNi panels with different passivations after 1000 hrs. in SST.

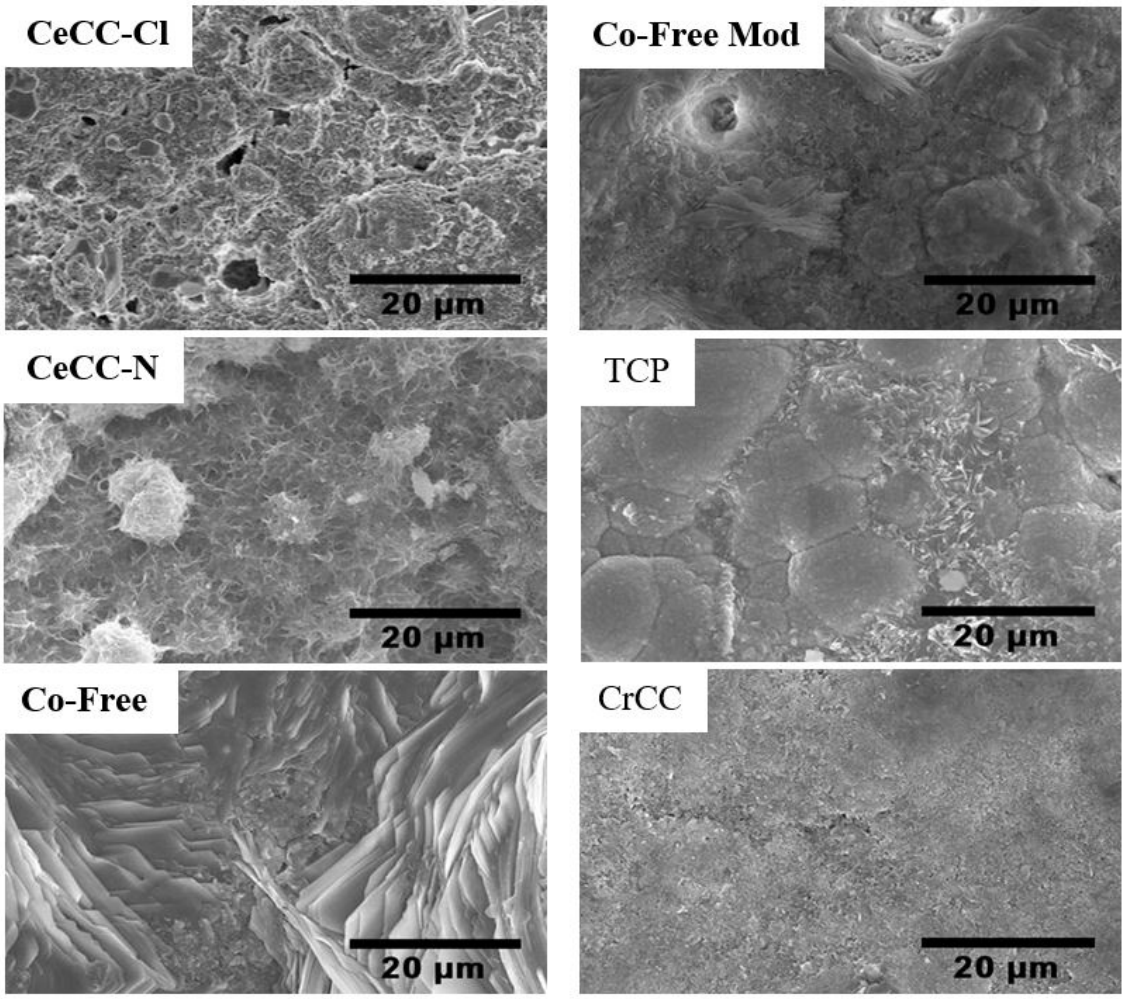

Figure 11: Surface morphology at 2000x of γ-ZnNi panels with different passivations after 1000 hrs. in SST.

like crystals. An extremely fine corrosion product was present on CrCC passivations, with a crystallite size of less than 500 nm. Some areas of TCP panels had corrosion product present, but the crystals were segregated to the grain boundaries of the γ-ZnNi coating. These crystals may grow near the grain boundaries due to higher surface energy in these areas, which could provide a more favorable area for growth. These results show how the passivation material can have a significant effect on the morphology of the corrosion product that forms during SST.

The chemical composition of corrosion products was examined by EDS, which revealed four major constituents, zinc, oxygen, chlorine, and nickel. Zinc and nickel were present in the electroplated ZnNi substrate, while chlorine was present in SST, which uses an aqueous NaCl solution. Oxygen must also be provided during SST, as the passivations could not possibly provide the levels of oxygen observed in the corrosion product. An apparent decrease in nickel content was observed for four of the six coating systems, with drops from 18 at% to 1 at% in the CeCCs, Co-Free, and CrCC coating systems. The Co-Free Mod and TCP coating systems had 6.8 and 11.3 at% nickel observed by EDS. The nickel content of the initial γ-ZnNi coating was around 18 at%. The apparent decrease in nickel content was likely due a combination of causes. The first was the thickness of the Zn-rich corrosion product layer, which would prevent the probe beam from reaching the underlying γ-ZnNi coating. Hence, passivations with higher apparent nickel contents had thinner corrosion product layers, which allowed signal from the probe beam to be detected. This assertion was made because both Co-Free Mod and TCP coating systems produced what visually looked to be the least amount of corrosion product in Figure 11 and, as shown in Table 1, both of these coating systems had significantly higher apparent nickel contents. The other potential mechanism for increasing the apparent Ni content is the mechanism by which the corrosion product was formed. During corrosion, zinc leaches out of the ZnNi coating and through the surface passivation, either through continuous microcracks or other imperfections in the passivations, or by the failure of the passivation. Once the zinc species are out of the coating system they can react to form zinc oxide corrosion complexes on the surface. Since none of the detected Ni contents are above the initial Ni content of the γ-

ZnNi coating, this latter mechanism seems unlikely to have affected the amount of Ni detected to a significant degree.

Table 1: Compositional analysis of the surface of γ-ZnNi after 1000 hrs. in SST.

(at%)	CeCC-Cl	CeCC-N	Co-Free	Co-Free Mod	TCP	CrCC
Zn	59.7	43.5	38.7	22.7	62.7	52.4
Ni	1.0	1.4	1.2	6.8	11.3	1.3
O	33.7	52.0	45.7	65.4	22	44.0
Fe	0.2	0.3	0.3		0.4	0.5
Cl	5.5	2.8	6.3		1.4	0.9
Cr				2.6	2.0	0.2
Co					0.3	
S			7.8	2.5		0.6
Al						0.2

The corroded panels were also examined using XRD, which showed the presence of zinc hydroxycarbonate, which is the expected corrosion product for zinc in a humid, oxidizing environment such as salt spray testing. Based on the microstructural analysis discussed above, the passivations affected the morphology of the product that developed on the surface of the panels during corrosion. Also, XRD allowed for comparison of the relative amounts of corrosion products. Based on lack of signal for Zn-rich species, formation of corrosion products was minimal on Co-Free Mod and TCP.

From another paper focusing on the electrochemical response of these coating systems, a relation between the microstructure and the EIS can be seen.[35] The TCP and Co-Free Mod passivations had distinctive differences compared to the other coating systems in their EIS responses and morphologies. Both the TCP and Co-Free Mod passivations had had a higher frequency response peak on the Bode phase angle plot at about 10 Hz compared to about 1 Hz for the rest of the passivations.[35] This difference means that the

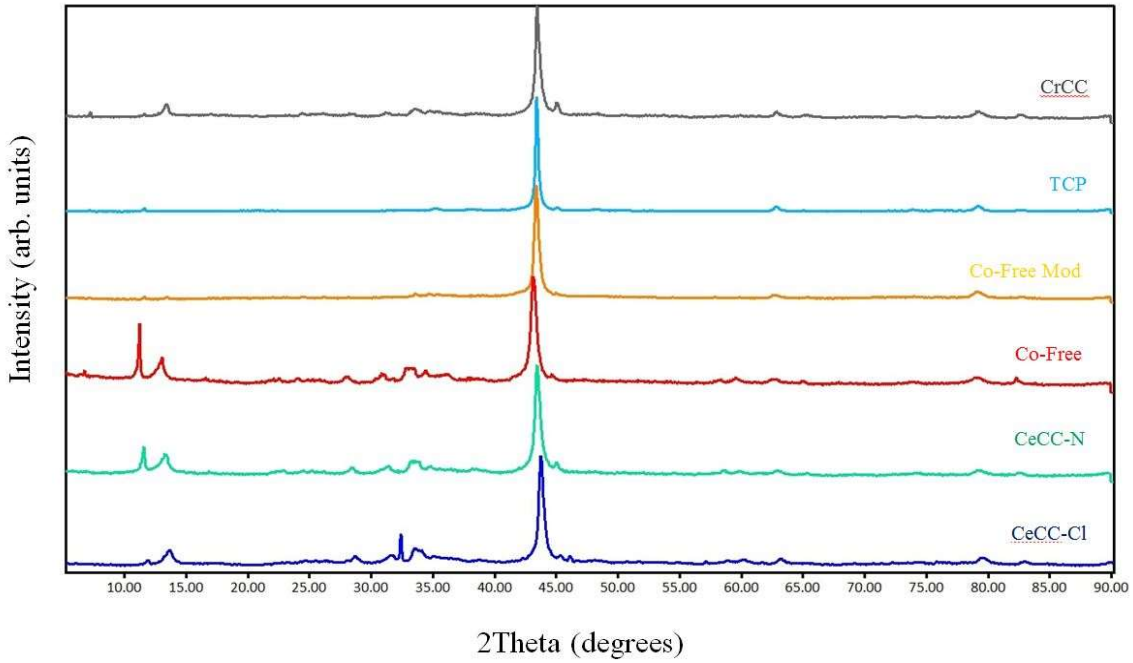

Figure 12: XRD of passivations on γ-ZnNi after 1000 hrs. in SST.

Table 2: Phase analysis of various passivations on γ-ZnNi after 1000 hrs. of SST. (Amount %)

	CeCC-Cl	CeCC-N	Co-Free	Co-Free Mod	TCP	CrCC
ZnNi	66.6	66.5	46.2	85.3	99.2	76.7
Corrosion Product	33.4	33.6	53.8	14.7	0.8	23.3

surfaces of the TCP and Co-Free Mod systems are electrochemically different compared to the rest of the systems. This electrochemical difference could be attributed to differences in the morphology of the surfaces. The most prominent difference being the lack of corrosion product seen on the surfaces of TCP and Co-Free Mod, seen in Figure 11. The corrosion product and passivations would have different electrochemical responses in EIS due to different chemical compositions. Also, noted from the other study is the electrical contact resistances observed.[35] Both TCP and Co-Free Mod coating systems had the lowest resistance values, which could also be attributed to the lack of corrosion product on the

surfaces of the passivations.[35] Due to the lack of corrosion product detected by materials characterization techniques XRD and SEM, and the electrochemical and electrical contact resistance results seen from another study using the same coating systems, the TCP and Co-Free Mod passivations, provided the best overall corrosion protection.

Conclusions

The composition and morphology were characterized for six different passivations on electroplated γ-ZnNi. The passivations had a significant impact on not only the amount of corrosion product that formed, but also the morphology of the corrosion products that developed during salt spray testing. The corrosion product was identified as zinc hydroxycarbonate by XRD. The Co-Free Mod and TCP passivations provided the most significant corrosion protection because these passivations were able to prevent the significant development of corrosion product, even when compared to the current industry standard of CrCC passivation on γ-ZnNi.

Acknowledgements

This work was funded by the Strategic Environmental Research and Development Program (SERDP) under contract. The support and guidance of Dr. Robin Nissan at SERDP is gratefully acknowledged. The authors would also like to thank Stephen Gaydos of Boeing for providing his expertise and Dr. Tarek Nahlawi of Dipsol of America for providing electroplated γ-ZnNi coatings on steel panels and many of the passivated panels. Finally, the authors are grateful for the use of the Advanced Materials Characterization Laboratory and the technical assistance of Dr. Eric Bohannan (XRD) and Dr. Clarrisa Wisner (SEM), all from the Missouri University of Science and Technology.

References

[1] A. Conde, M.A. Arenas, J.J. Damborenea, Corrosion Science 53 (2011) 1489-1497.

[2] Guenter Schmitt, Tim Gommlich, K. Schottler, N. International, Corrosion 2014, NACE International, San Antonio, Texas, 2014.

[3] K. R. Baldwin, M. J. Robinson, C.J.E. Smith, Corrosion Science 35 (1993) 1297-1272.

[4] Moonjae Kwon, Soo Hyoun Cho, Yuan Tae Kim, Jong-Tae Park, J.M. Park, Surface & Coating Technology 288 (2016) 163-170.

[5] R. Ramanauskas, L. Gudaviciute, L. Diaz-Ballote, P. Bartolo-Perez, P. Quintana, Surface & Coating Technology 140 (2001) 109-115.

[6] Tom Naguy, George Slenski, Robert Keenan, G. Chiles, Replacement Coatings For Aircraft Electronic Connectors: Findings And Potential Alternatives Report, in: D.o. Defense (Ed.) 1998.

[7] D.o. Defense, MIL-DTL-38999M, 2015.

[8] Johannes Godt, Franziska Scheidig, Christian Grosse-Siestrup, Vera Esche, Paul Brandenburg, Andrea Reich, D.A. Groneberg, Journal of Occupational Medicine and Toxicology (2006).

[9] Donald A. Wright, N. Gage, Transactions of the Insitute of Metal Finishing 72(4) (1994) 130-133.

[10] A.Y. Polyakov, N.B. Smirnov, A.V. Govorkov, E.A. Kozhukhova, S.J. Pearton, D.P. Norton, A. Osinsky, A. Dabiran, Journal of Electronic Materials 35(4) (2006) 663-669.

[11] S.C. Gad, The Science of the total enviroment 86(1-2) (1989) 149-157.

[12] Becky L. Treu, Simon Joshi, William R. Pinc, Matthew J. O'Keefe, W.G. Fahrenholtz, Journal of the Electrochemical Society 157(8) (2010) C282-C287.

[13] Carlos E. Castano, Matthew J. O'Keefe, W.G. Fahrenholtz, Current Opinion in Solid State and Material Science 19 (2015) 69-76.

[14] Daimon K. Heller, William G. Fahrenholtz, M.J. O'Keefe, Journal of the Electrochemical Society 156 (2009) C400-C406.

[15] William G. Fahrenholtz, Matthew J.O'Keefe, Haifeng Zhou, J.T. Grant, Surface & Coating Technology 155 (2002) 208-213.

[16] K. Aramaki, Corroison Science 43 (2001) 2201-2215.

[17] Carlos E. Castano, Surender Maddela, M.J. O'Keefe, Magnesium Technology (2013) 169-172.

[18] Simon Joshi, Elizabeth, A. Kulp, William G. Fahrenholtz, M.J. O'Keefe, Corrosion Science (60) (2012) 290-295.

[19] T.J. Haley, Journal of Pharmaceutical Sciences 54(5) (1965) 663-670.

[20] Yuanyuan Liu, Jiamu Huang, James B. Claypool, Carlos E. Castano, M.J. O'Keefe, Surface Engineering 355 (2015) 805-813.

[21] A. Aballe, M. Bethencourt, F. J. Botana, M.J. Cano, M. Marcos, Materials and Corrosion 53 (2002) 176-184.

[22] M. G. Hosseini, H. A. Y. Ghiasvand, H. Ashassi-Sorkhabi, Surface Engineering 29(1) (2013).

[23] KuenWoo Cho, V. Shankar Rao, H. Kwon, Electrochimica Acta (52) (2007) 4449-4456.

[24] Robert Berger, B. Ulf, T. Mikeal Grehk, S.-E. Hornstrom, Surface & Coating Technology (202) (2007) 391-397.

[25] X. Zhang, C. van den Bos, W.G. Sloof, A. Hovestad, H. Terryn, J.H.W.d. Wit, Surface & Coating Technology (199) (2005) 92-104.

[26] A. Gardner, J. Scharf, Transactions of the Insitute of Metal Finishing 81(6) (2003) B107-B111.

[27] Ahmed Elbetieha, M.H. Al-Hamood, Toxicology 116 (1997) 39-47.

[28] T. Bellezze, G. Roventi, R. Fratesi, Surface & Coating Technology 155 (2002) 221-230.

[29] Niann-Tsyr Wen, Chao-Sung Lin, Ching-Yuan Bai, M.-D. Ger, Surface and Coatings Technology (203) (2008) 317-323.

[30] Vanessa de Freitas Cunha Lins, Geraldo Francisco de Andrade Reis, Carlos Roberto de Araujo, T. Matencio, Applied Surface Science 253 (2006) 2875-5884.

[31] Soroor Ghaziof, W. Gao, Applied Surface Science 311 (2014) 635-642.

[32] M. Cymboliste, journal of the Electrochemical Society 70(1) (1936) 379-396.

[33] B.R. Hinderliter, S.G. Croll, D.E. Tallman, Q. Su, G.P. Bierwagen, Electrochimica Acta 51 (2006) 4505-4515.

[34] A. Johansson, H. Ljung, S. Westman, Acta Chemica Scandinavica 22 (1968) 2743-2753.

[35] S.M. Volz, J.B. Claypool, M.J. O'Keefe, W.G. Fahrenholtz, 3. Corrosion Behavior and Contact Resistance of electroplated γ-ZnNi with Passivation layers, Material Science and Engineering, Missouri University of Science and Technology, 2017.

SECTION

3. CONCLUSIONS

Six different passivations, two CeCC based, three TCP based, and a CrCC, were deposited on electroplated, low hydrogen embrittlement γ-phase zinc nickel alloy on steel. The CrCC coating was used a reference to compare the CeCC-Cl, CeCC-N, Co-Free, Co-Free Mod, and TCP coating systems. Analysis of the data generated leads to the following conclusions:

- All coating systems can produce an as-deposited electrical contact value below the required value of 0.8 $m\Omega/cm^2$.
- The electrochemically active coatings with more negative open circuit potential, being the chromium-based passivations, provided the best corrosion response in SST.
- Coatings with a higher frequency peak value after SST on the Bode phase angle plot had better corrosion resistance.
- The chemical composition of the corrosion product on all coating systems was found to best match zinc hydroxycarbonate crystal structures.
- The morphology of the corrosion product was dependent on the passivation layer.
- After 1000 hrs. of SST, both TCP and Co-Free Mod had an electrical contact resistance able to achieve the 1.6 $m\Omega/cm^2$ specification value for DoD connectors.

- This research found that the TCP based coating systems had better corrosion performance on γ-ZnNi than the CeCC based coating systems investigated.

4. FUTURE WORK

Future plans should include further testing of TCP and Co-Free Mod coating systems as well as reproducing the results seen in the SST experiment. Transmission Electron Microscopy (TEM) analysis or profilometry experiments should be considered to get more accurate thicknesses of the passivations as well as examining the changes in passivations during SST. The experiments could be reproduced on varying surface finishes this would help determine proper deposition conditions and to develop a more accurate electrical resistance measurement. Cerium-based passivations could also be deposited by electrodeposition or spray deposition to see if that has an effect on the end results. Evaluation of electrical connectors is needed, with the passivation systems and following the rigorous testing outlined in MIL-DTL-38999, to determine if the passivation is acceptable for commercial use in this application. Other environmentally friendly passivation alternatives should be explored. The development of a better electrical contact resistance test method could improve the accuracy and reproducibility of the measurements.

BIBLIOGRAPHY

Introduction

[1] Tom Naguy, George Slenski, Robert Keenan, G. Chiles, D.o. Defense (Ed.) 1998.

[2] X. Zhang, C. van den Bos, W.G. Sloof, A. Hovestad, H. Terryn, J.H.W.d. Wit, Surface Engineering 20(4) (2004) 244-250.

[3] M. G. Hosseini, H. A. Y. Ghiasvand, H. Ashassi-Sorkhabi, Surface Engineering 29(1) (2013).

Literature Review

[1] K.N. Rao, M.I.A. Siddiqi, C.V. Suryanarayana, Electrochimica Acta 10(6) (1965) 557-562.

[2] A. Komoda, A. Matsuda, T. Yoshihara, H. Kimura, AES Fourth Continuous Strip Plating Symposium, Chicago, IL, USA, 1984.

[3] D.E. Hall, Plating and Surface Finishing 70(11) (1983) 59-65.

[4] G.D. Wilcox, D.R. Gabe, Corrosion Science 35(5-8) (1993) 1251-1258.

[5] P. Nash, Y.Y. Pan, Bulletin of Alloy Phase Diagrams 8(5) (1987) 422-430.

[6] E.W. Horvick, Zinc, Properties and Selection: Nonferrous Alloys and Special-Purpose Materials, in: D.H. Nevison (Ed.) ASM Handbook, 1990, pp. 1099-1201.

[7] R.J. Barnhurst, Zinc and Zinc Alloys, Properties and Selection: Nonferrous Alloys and Special-Purpose Materials, ASM Handbook, 1990, pp. 527-542.

[8] K.R. Sriaman, S. Brahimi, J.A. Szpunar, J.H. Osborne, S. Yue, Surface & Coating Technology 224 (2013) 126-137.

[9] Chuen-Chang Lin, C.-M. Huang, JCT Research 3(2) (2006) 99-104.

[10] S.H. Mosavat, M.H. Shariat, M.E. Bahrololoom, Corrosion Science 59 (2012) 81-87.

[11] C. Bowden, A. Matthews, Surface & Coating Technology 76-77 (1995) 508-515.

[12] R. Fratesi, G. Roventi, Journal of Applied Electrochemistry 22 (1992) 657-662.

[13] Soroor Ghaziof, W. Gao, Applied Surface Science 311 (2014) 635-642.

[14] Johannes Godt, Franziska Scheidig, Christian Grosse-Siestrup, Vera Esche, Paul Brandenburg, Andrea Reich, D.A. Groneberg, Journal of Occupational Medicine and Toxicology (2006).

[15] K. R. Sriraman, S. Branhimi, J.A. Szpunar, journal of Applied Electrochemistry 43 (2013) 441-451.

[16] M.R. Louthan Jr., G.R. Caskey Jr., J.A. Donovan, D.E.R. Jr., Materials Science and Engineering 10 (1972) 357-368.

[17] R.A. Oriani, Acta Metallurgica 18 (1970) 147-157.

[18] Donald A. Wright, N. Gage, Transactions of the Institute of Metal Finishing 72(4) (1994) 130-133.

[19] A. Conde, M.A. Arenas, J.J. Damborenea, Corrosion Science 53 (2011) 1489-1497.

[20] K. R. BALDWIN, M. J. ROBINSON, C.J.E. SMITH, Corrosion Science 35 (1993) 1297-1272.

[21] Moonjae Kwon, Soo Hyoun Cho, Yuan Tae Kim, Jong-Tae Park, J.M. Park, Surface & Coating Technology 288 (2016) 163-170.

[22] Hany M. ABD EL-LATEEF, Abdel-Rahman El-Sayed, H.S. Mohran, Transactions of the Nonferrous Metal Society 25 (2015) 2807-2816.

[23] Prabhu Ganesan, Swaminatha P. Kurmaraguru, B.N. Popov, Surface & Coating Technology 201 (2007) 7896-7904.

[24] P. Pokorny, P. Tej, P. Szelag, METABK 55(2) (2016) 253-256.

[25] X. Zhang, C. van den Bos, W.G. Sloof, A. Hovestad, H. Terryn, J.H.W.d. Wit, Surface Engineering 20(4) (2004) 244-250.

[26] X. Zhang, C. van den Bos, W.G. Sloof, A. Hovestad, H. Terryn, J.H.W.d. Wit, Surface & Coating Technology (199) (2005) 92-104.

[27] B. R. W. Hinton, D. R. Arnott, N.E. Ryan, Material Forum 9(3) (1986) 162-173.

[28] F.H. Scholes, C. Soste, A.E. Hughes, S.G. Hardin, P.R. Curtis, Applied Surface Science 253 (2006) 1770-1780.

[29] M. Kendig, S. Jeanjaquet, R. Addison, J. Waldrop, Surface & Coating Technology 140 (2001) 58-66.

[30] Yu-Tsern Chang, Niann-Tsyr Wen, We-Kun Chen, Ming-Der Ger, Guan-Tin Pan, T.C.-K. Yang, Corroison Science 50 (2008) 3494-3499.

[31] Lin Xia, R.L. McCreery, Journal of the Electrochemical Society 145(9) (1998) 3083-3089.

[32] A.E. Hughes, R.J. Taylor, B.R.W. Hinton, Surface and Interface Analysis 25 (1997) 223-234.

[33] M.W. Kendig, R.G. Buchheit, Corrosion Science 59(5) (2003) 379-400.

[34] E. Akiyama, A. J. Markworth, J. K. McCoy, G. S. Frankel, L. Xia, R.L. McCreery, Journal of the Electrochemical Society 150(2) (2003) B83-B91.

[35] J. Zhao, L. Xia, A. Sehgal, D. Lu, R.L. McCreery, G.S. Frankel, Surface & Coating Technology 140 (2001) 51-57.

[36] S.C. Gad, The Science of the total environment 86(1-2) (1989) 149-157.

[37] Ahmed Elbetieha, M.H. Al-Hamood, Toxicology 116 (1997) 39-47.

[38] N.T. Wen, F.J. Chen, M.D. Ger, Y.N. Pan, C.S. Lin, Electrochemical and Solid State Letters 11(8) (2008) C47-C50.

[39] KuenWoo Cho, V. Shankar Rao, H. Kwon, Electrochimica Acta (52) (2007) 4449-4456.

[40] Niann-Tsyr Wen, Chao-Sung Lin, Ching-Yuan Bai, M.-D. Ger, Surface and Coatings Technology (203) (2008) 317-323.

[41] H. Bhatt, Trivalent Chromium Conversion Coating for Corrosion Protection of Aluminum Surface, 2009 DoD Corrosion Conference, METALAST International, Inc., 2241Park Place, Suite C, Minden, NV 89423, 2009.

[42] A. Gardner, J. Scharf, Transactions of the Institute of Metal Finishing 81(6) (2003) B107-B111.

[43] L.M. Baugh, Electrochimica acta 24(6) (1979) 657-667.

[44] L. Fedrizzi, L. Ciaghi, P. L. Bonora, R. Fratesi, G. Roventi, Journal of Applied Electrochemistry 22(3) (1992) 247-254.

[45] T.J. Haley, Journal of Pharmaceutical Sciences 54(5) (1965) 663-670.

[46] Shujiang Geng, Pu Yu, Matthew J. O'Keefe, William G. Fahrenholtz, T.J. O'Keefe, Journal of Applied Electrochemistry 40 (2010) 551-559.

[47] Becky L. Treu, Simon Joshi, William R. Pinc, Matthew J. O'Keefe, W.G. Fahrenholtz, Journal of the Electrochemical Society 157(8) (2010) C282-C287.

[48] Daimon K. Heller, William G. Fahrenholtz, M.J. O'Keefe, Journal of the Electrochemical Society 156 (2009) C400-C406.

[49] Daimon K. Heller, William G. Fahrenholtz, M.J. O'Keefe, Corrosion Science 52 (2010) 360-368.

[50] W. Pinc, P. Yu, M. O'Keefe, W. Fahrenholtz, Surface & Coating Technology 203 (2009) 3533-3540.

[51] W. Pinc, S. Geng, M. O'Keefe, W. Fahrenholtz, T. O'Keefe, Applied Surface Science 255 (2009) 4061-4065.

[52] Andre Decroly, J.-P. Petitjean, Surface & Coating Technology 194 (2005) 1-9.

[53] K. Aramaki, Corrosion Science 43 (2001) 2201-2215.

[54] M. G. Hosseini, H. A. Y. Ghiasvand, H. Ashassi-Sorkhabi, Surface Engineering 29(1) (2013).

[55] William G. Fahrenholtz, Matthew J.O'Keefe, Haifeng Zhou, J.T. Grant, Surface & Coating Technology 155 (2002) 208-213.

[56] Yanchun Zhou, J.A. Switzer, Journal of Alloys and Compounds 237 (1996) 1-5.

[57] C.S. Lin, S.K. Fang, Journal of the Electrochemical Society 152(2) (2005) B54-B59.

[58] Carlos E. Castano, Surender Maddela, M.J. O'Keefe, Magnesium Technology (2013) 169-172.

[59] Manuele Dabala, Katya Brunelli, Enrico Napolitani, M. Magrini, Surface & Coating Technology 172 (2003) 227-232.

[60] Simon Joshi, Elizabeth, A. Kulp, William G. Fahrenholtz, M.J. O'Keefe, Corrosion Science (60) (2012) 290-295.

[61] D.o. Defense, MIL-DTL-38999M, 2015.

[62] H.L.J. Archer, W.J. Powell, J.T. Menke, Method for deposition of steel protective coating, United States 2009.

[63] R. Misiaszek, Alternatives to Cadmium Plated Military Connectors and Fasteners, Aerospace/Defense Industry Supply Chain Conference: Chemicals of Concern and Safer Solutions, Strurbridges, MA, USA, 2013.

[64] M. Neidbalson, Development of Cadmium and Hexavalent Chromium Free Electrical Connectors: Test Results, in: D.o. Defense (Ed.) NDIA Environment, Energy Security & Sustainability (E2S2) Symposium & Exhibition, 2010.

[65] L. Kogut, K. Komvopoulos, Journal of Applied Physics 95 (2004) 576-585.

[66] D.o. Defense, MIL-DTL-81706A, 2002.

[67] C. Matzdorf, Non-chromate Aluminum Pretreatments Phase I Report, in: E.S.T.C. Program (Ed.) NCAP Phase I Report, 2003.

[68] Bryson J. Lanterman, Adriaan A. Riet, Nathaniel S. Gates, Joshua D. Flygare, Andrew D. Cutler, Dean R. Wheeler, B.A. Mazzeo, Journal of the Electrochemical Society 162(10) (2015) A2145-A2151.

[69] Joshua D. Flygare, Adriaan A. Riet, Brian A. Mazzeo, D.R. Wheeler, Journal of the Electrochemical Society 162(10) (2015) A2136-A2144.

VITA

Steven Michael Volz was born on January 9th, 1993 in St. Peters, MO. In August of 2011, Steven started his undergraduate degree in Ceramic Engineering at Missouri University of Science and Technology in Rolla, MO. During his time as an undergraduate Steven worked on research projects under graduate student Ali Mohammadkhah. These projects included working with bio-glass and nuclear waste glass systems. He also joined Material Advantage and Keramos, during this time. During the school year from fall 2014 to spring 2015 Steven held the position of Nomination Chair on the executive board and website committee lead in Keramos. Steven graduated cum laude from Missouri University of Science and Technology with a B.S. degree in Ceramic Engineering in May of 2015.

Steven also began to pursue his Master's degree in Materials Science and Engineering at Missouri University of Science and Technology, in May of 2015 under his advisors, Dr. Matthew O'Keefe and Dr. William Fahrenholtz. During his graduate career, Steven researched passivation layers on electroplated γ-ZnNi for use in DOD electrical systems. He also gave two presentations at different conferences while in graduate school and joined the Alpha Sigma Mu Professional Fraternity. Steven received his M.S. degree in Materials Science and Engineering from Missouri University of Science and Technology in May of 2017.